AD-A143 542 LOSS FACTORS MEASURED IN METAL MATRIX COMPOSITE MATERIALS(U) BOLT BERANEK AND NEWMAN INC CAMBRIDGE MA N S TIMMERMAN ET AL. JUN 84 BBN-5520 AMMRC-TR-84-22 1/1

UNCLASSIFIED DAAG46-82-C-0060 F/G 11/4 NL

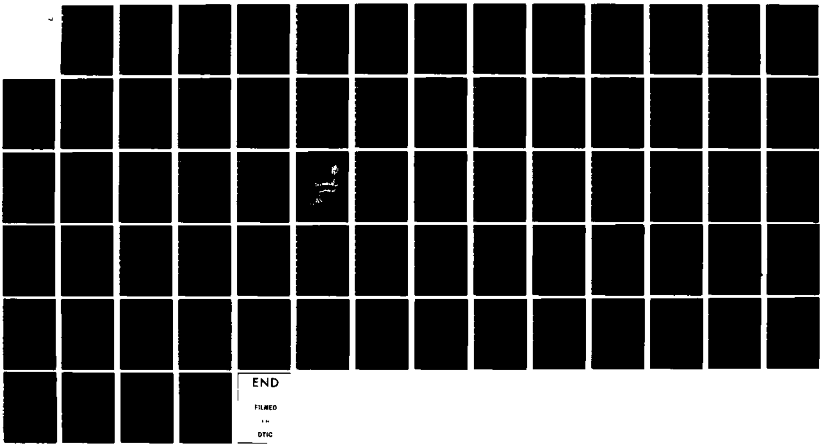

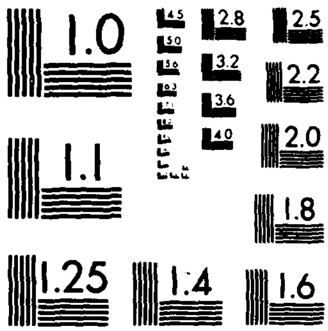

MICROCOPY RESOLUTION TEST CHART
NATIONAL BUREAU OF STANDARDS-1963-A

6

AD

AMMRC TR 84-22

LOSS FACTORS MEASURED IN METAL MATRIX COMPOSITE MATERIALS

June 1984

NANCY S. TIMMERMAN and JOHN DOHERTY
Bolt Beranek and Newman Inc.
10 Moulton Street
Cambridge, Massachusetts 02138

FINAL REPORT

Contract No. DAAG46-82-C-0060

Approved for public release; distribution unlimited.

Prepared for

ARMY MATERIALS AND MECHANICS RESEARCH CENTER
Watertown, Massachusetts 02172

AD

AMMRC TR 84-22

LOSS FACTORS MEASURED IN METAL MATRIX COMPOSITE MATERIALS

June 1984

NANCY S. TIMMERMAN and JOHN DOHERTY
Bolt Beranek and Newman Inc.
10 Moulton Street
Cambridge, Massachusetts 02138

FINAL REPORT

Contract No. DAAG46-82-C-0060

Approved for public release; distribution unlimited.

Prepared for

ARMY MATERIALS AND MECHANICS RESEARCH CENTER
Watertown, Massachusetts 02172

DISPOSITION INSTRUCTIONS

Destroy this report when it is no longer needed
Do not return it to the originator.

UNCLASSIFIED

SECURITY CLASSIFICATION OF THIS PAGE (When Data Entered)

REPORT DOCUMENTATION PAGE		READ INSTRUCTIONS BEFORE COMPLETING FORM
1. REPORT NUMBER AMMRC TR 84-22	2. GOVT ACCESSION NO. AD-A143542	3. RECIPIENT'S CATALOG NUMBER
4. TITLE (and Subtitle) LOSS FACTORS MEASURED IN METAL MATRIX COMPOSITE MATERIALS -		5. TYPE OF REPORT & PERIOD COVERED Final Report - 14 Sept. 82 through 30 Nov. 83
		6. PERFORMING ORG. REPORT NUMBER 5520
7. AUTHOR(s) Nancy S. Timmerman and John Doherty		8. CONTRACT OR GRANT NUMBER(s) DAAG46-82-C-0060
9. PERFORMING ORGANIZATION NAME AND ADDRESS Bolt Beranek and Newman Inc. 10 Moulton Street Cambridge, Massachusetts 02138		10. PROGRAM ELEMENT, PROJECT, TASK AREA & WORK UNIT NUMBERS D/A Project: 1L263102D071 Agency Accession: DA OG4061
11. CONTROLLING OFFICE NAME AND ADDRESS Army Materials and Mechanics Research Center ATTN: DRXMR-K Watertown, Massachusetts 02172		12. REPORT DATE June 1984
		13. NUMBER OF PAGES 64
14. MONITORING AGENCY NAME & ADDRESS(if different from Controlling Office)		15. SECURITY CLASS. (of this report) Unclassified
		15a. DECLASSIFICATION/DOWNGRADING SCHEDULE
16. DISTRIBUTION STATEMENT (of this Report) Approved for public release; distribution unlimited.		
17. DISTRIBUTION STATEMENT (of the abstract entered in Block 20, if different from Report)		
18. SUPPLEMENTARY NOTES		
19. KEY WORDS (Continue on reverse side if necessary and identify by block number) Metal matrix composites Damping Graphite	Alumina Silicon oxides Magnesium	Aluminum Resonance Loss factor
20. ABSTRACT (Continue on reverse side if necessary and identify by block number) (SEE REVERSE SIDE)		

DD FORM 1 JAN 73 1473 EDITION OF 1 NOV 65 IS OBSOLETE

UNCLASSIFIED

SECURITY CLASSIFICATION OF THIS PAGE (When Data Entered)

Block No. 20

ABSTRACT

The resonant dwell technique was used to measure loss factors at the fundamental frequency of a number of cantilever beam samples (100 to 200 Hz). Nine different metal matrix composites, three unreinforced base metals, and eight configurations of FP(Al_2O_3)/ZE41AMg were tested at three temperatures and four peak sample stress levels below 30,000 psi. The results indicate increasing loss factor with increasing stress level. Loss factors of all composites except graphite/aluminum composites were lower than those of the corresponding base metal. For FP/ZE41AMg composites, higher losses were observed with heat treatment, lower fiber volume fraction, and $\pm 22\text{-}1/2^{\circ}$ fiber orientation. Trends of loss factor with temperature varied with material type.

FOREWORD

This is the Final Report on BBN Job Number 07529, "Damping Characteristics of Metal Matrix Composites," prepared by BBN for the Army Materials and Mechanics Research Center (AMMRC) under Contract Number DAAG-46-82-C-0060. The work described in this report was conducted in the period 14 September 1982 through 30 November 1983. Mr. John Nunes was the Technical Monitor for AMMRC. The BBN personnel who contributed to this program include Drs. E. Ungar and J. Heine, Messrs. J. Doherty and F. Iacovino, and Ms. N. Timmerman.

Respectfully submitted,
BOLT BERANEK AND NEWMAN INC.

Nancy S. Timmerman
Senior Engineer

APPROVED:

Francis J. Jackson
Senior Vice President
BBN Laboratories

NT/gh

ABSTRACT

LOSS FACTORS MEASURED IN METAL MATRIX COMPOSITE MATERIALS

The resonant dwell technique was used to measure loss factors at the fundamental frequency of a number of cantilever beam samples (100 to 200 Hz). Nine different metal matrix composites, three unreinforced base metals, and eight configurations of FP(AL_2O_3)/ZE41AMg were tested at three temperatures and four peak sample stress levels below 30,000 psi. The results indicate increasing loss factor with increasing stress level. Loss factors of all composites except graphite/aluminum composites were lower than those of the corresponding base metal. For FP/ZE41AMg composites, higher losses were observed with heat treatment, lower fiber volume fraction, and $\pm 22\frac{1}{2}^{\circ}$ fiber orientation. Trends of loss factor with temperature varied with material type.

+ or - $22\frac{1}{2}$ °

TABLE OF CONTENTS

1. INTRODUCTION

In this project, the stress and temperature dependence of the material loss factor in nine metal matrix composite materials, eight varieties of FP(Al_2O_3)/ZE41A Magnesium, and three unreinforced base metals were studied. The test method used was developed by Heine in the 1960's and is known as the Resonant Dwell Technique. Each cantilever beam sample was tested at its fundamental resonant frequency (between 100 and 200 Hz), at four(4) different peak sample stress levels (between 5000 and 30,000 psi), and at one of three temperatures (room temperature, 200° F, or 400° F).

The program was divided into two phases. In the first phase, the same nine composite materials which had been used in a previous study [1] were tested, as were the three unreinforced matrix alloys. In the second phase, only the FP(Al_2O_3)/ZE41A Mg composites were evaluated for the following conditions: volume fraction of the FP fiber (35% or 55%), orientation of the FP fibers with respect to the axis of bending (0° or $\pm 22\frac{1}{2}^\circ$), and heat treatment of the composite (as cast or T-5).

The following sections discuss the test specimens used, the experimental test procedures followed, and the results obtained. Problems encountered, and the significance of the data obtained are also discussed, along with recommendations for future work.

2. DISCUSSION

2.1 Test Specimens

2.1.1 Materials used in phase 1

The materials tested in Phase 1 consisted of three base metals (6061 Aluminum, ZE41A Magnesium, and Commercially Pure Magnesium), and the nine metal matrix composites which had been previously studied under Contract Number DAAG-46-81-C-0036 [1]. The specimens were all furnished by AMMRC.

The nine metal matrix composite materials were:

1. Graphite/Aluminum: The graphite fibers were of pitch precursor type, with a modulus of 55 Msi. The aluminum alloy was 6061.

2. Graphite/Aluminum: The graphite fibers were of pitch precursor type, with a modulus of 100 Msi. The aluminum alloy was 6061.

3. Graphite/Magnesium: The graphite fibers were of pitch precursor type, with a modulus of 55 Msi. The magnesium alloy was ZE41A.

4. Graphite/Magnesium: The graphite fibers were of the pitch precursor type, with a modulus of 100 Msi. The magnesium alloy was ZE41A.

5. FP/Aluminum: FP was Al_2O_3 fiber. The aluminum alloy was aluminum with 2% lithium.

6. FP/Magnesium: FP was Al_2O_3 fiber. The magnesium alloy was ZE41A.

7. FP/Magnesium: FP was Al_2O_3. The magnesium matrix was commercially pure magnesium.

8. SiC/Aluminum: The silicon carbide was in particulate form with a volume fraction of 45%. The aluminum alloy was 6061.

9. SiC/Aluminum: The silicon carbide was in whisker form with a volume fraction of 20%. The aluminum alloy was 6061.

Materials 1 through 7 contained continuous reinforcing fibers, oriented parallel to the longest dimension of the cantilever beam specimens, with a volume fraction of 50 ± 5%.

Each material was represented by three identical cantilever beam specimens. The specimen dimensions are given in Figure 1. For each of the three base metals, the beam length, L_s, was 4 3/4 inches, while for each of the nine composite materials it was 6 inches. Representative values for material density and Young's modulus (parallel to the fiber direction for continuous fibers) are given in Table 1.

2.1.2 Materials used in Phase 2

The materials tested in Phase 2 consisted of eight configurations of FP(Al_2O_3)/ZE41A Magnesium composites of varying fiber content, fiber orientation, and heat treatment. In all cases the fiber was polycrystalline Al_2O_3 and the samples were obtained from DuPont Textile Fibers Department. The T-5 heat treatment was provided by Industrial Heat Treating, Inc. in Massachusetts, and certification is given in Appendix A. The eight configurations were:

1. 35% volume fraction (v/o) of FP at 0° fiber orientation (parallel to the longest dimension of the samples). As cast.
2. 35% v/o FP at 0° fiber orientation. T-5 heat treated.
3. 35% v/o FP at $\pm 22\frac{1}{2}^\circ$ fiber orientation. As cast.
4. 35% v/o FP at $\pm 22\frac{1}{2}^\circ$ fiber orientation. T-5 heat treated.

5. 56% v/o FP at 0° fiber orientation. As cast.

6. 56% v/o FP at 0° fiber orientation. T-5 heat treated.

7. 56% v/o FP at $\pm 22\frac{1}{2}^{\circ}$ fiber orientation. As cast.

8. 56% v/o FP at $\pm 22\frac{1}{2}^{\circ}$ fiber orientation. T-5 heat treated.

Each material was represented by six identical cantilever beam specimens. In each case, the beam length, L_s, was 6 inches. All other dimensions were as in Figure 1. Representative values of material density, Young's modulus, and longitudinal tensile strength are given in Table 2 for the twelve material lots tested.

2.2 Test Methods

2.2.1 Resonant dwell technique

The resonant dwell technique is a forced vibration method of indirectly determining the loss factors of simple structural elements (usually cantilever beams) by measuring their response to excitation at a modal frequency. The method has been used at MIT by Granick & Stern [2], Heine [3], and Grau [4], at the University of Minnesota by Plunkett and Sax [5], and at the University of Idaho by Gibson, Yau and Riegner [6], as well as at BBN.

Using this test, the specimen loss factor at a mode (usually the fundamental) is determined from the resonant amplification factor, or Q, of the specimen in that mode. The mechanical Q of a vibrating system is defined in terms of a characteristic deflection δ of the system due to distributed exciting forces proportional to the inertia forces of the mode in question. The amplification factor at resonance is

$$Q = \frac{\delta_{res}}{\delta_0}$$

where δ_0 is the deflection due to the distributed exciting force being applied statically and δ_{res} is the deflection when the same pattern of forces is applied in simple harmonic motion at the modal natural frequency. The relationship between Q, the specimen loss factor η, and the logarithmic decrement Δ of single-degree-of-freedom system is

$$\Delta = \frac{\pi}{Q} = \pi\eta \ .$$

Note that higher loss factors thus represent lower Q's or higher damping capacities.

The particular technique used in this study is a single cantilever beam mounted as a vibration absorber, and is the method used by Heine. Figure 2 shows the essentials of the apparatus. A force is applied to the bottom of a "hinge," which acts as the first spring-mass system. At a natural frequency of the beam, the input vibrational energy is "absorbed" by the sample and the motion of the "hinge" is a minimum. At this response minimum, the resonance condition of the beam, the specimen tip displacement, x(t), is measured optically. The response of the supporting system, y(t), is measured with an accelerometer mounted near the root of the specimen.

Details of the experimental arrangement are shown in Figures 3 and 4. The driving force is applied by a shaker which is isolated from the rest of the supporting structure. The "hinge" consists of a bar (B) whose thickness at the base-attachment end has been reduced by a saw cut to provide a pivot around which the remainder of the bar can rotate when excited by the shaker. The test specimen is clamped to the top of the "hinge," and a response accelerometer is mounted on the clamp at the root of the specimen. The shaker is connected to the "hinge" by a rod which passes through a hole in the heavy base to which the rest of the supporting structure is attached.

The specimen loss factor is calculated from measurements of the root acceleration at a beam resonance. The resonance frequency is determined by adjusting the shaker forcing frequency until the root accelerometer output is a minimum. Away from resonance, the sample tip displacement, monitored with an optical microscope (with reticle) and a stroboscope, is kept below the desired level. Near the resonance frequency, the tip displacement is then adjusted for the desired peak sample stress (which occurs at the root). That double-amplitude tip displacement is determined from beam dimensions and material properties, as shown in Appendix B. The root acceleration then is measured and used to calculate the loss factor as follows [3]:

$$\eta = 0.083\ (1 + 0.2\ L)\ \frac{a_0}{f_n^2}\ \frac{1}{Y_{t,DA}}$$

where η is the specimen loss factor, f_n is the natural frequency (Hz), $Y_{t,DA}$ is the double amplitude tip displacement (inches), a_o is the root acceleration (in/sec), and L is the specimen length (inches). Note that Y_t,DA is just twice δ_{res} when measured at the tip of the specimen.

The advantages of using the resonant dwell method are several. First, the ratio δ_0/δ_{res}, for a properly designed specimen, is dependent only upon the damping in the specimen. Second, the vibration amplitude δ_{res} may be maintained at any constant level so that specimen damping may be determined as an *increasing* function of stress, eliminating the possibility of stress history effects. Third, because nothing is attached directly to the vibrating specimen, extraneous losses are minimized. Finally, the equipment is simple and the samples small enough to enclose in a temperature chamber, so that damping may be determined as a function of temperature.

None of our tests were run in a vacuum. Extraneous losses may occur due to air damping. Therefore, some estimates were made of the expected magnitude of the air damping for these specimens. The estimates were based on the work of Heine [3] [7] and Grau [4]. In these reports, the air damping, η_a, was given by:

$$\eta_a = \frac{\rho_a}{\rho} \frac{\delta_{res}}{h} C_D^*$$

where ρ_a = density of air, ρ = density of beam material, δ_{res} = displacement amplitude of the beam tip, h = thickness of the beam, and C_D^* is a dimensionless drag coefficient experimentally found to be a constant.

Thus, in this study, we assume C_D^* to be a constant for each temperature used, with material and sample shape dependence as given above. We thus found an upper bound on C_D^* from the smallest measured total values of η_a. The values of C_D^* used here were .8400 at room temperature, .618 at 200° F and .5698 at 400° F. These compare with experimental values reported at $.33 \leq C_D^* \lesssim 1$. An upper bound on η_a was then computed for each sample based on these maximum values of C_D^*. Corrected values of η were then computed with the assumption that

$$[\eta \text{ (measured)} = \eta + \eta_a].$$

2.2.2 Stress and temperature tests

Each sample was tested at one temperature and at four stress levels between 5000 and 30,000 psi in both phases of this study. The samples were individually identified by material type and piece number, so that, for example, sample D-12 was material D (56 v/o FP/ZE41A at 0° orientation), piece number 12. The individual samples were allocated among the three temperatures to give a complete, uniform set of data (see Table 3). In Phase 1, one sample of each material was tested at each of the three temperatures, while in Phase 2, two samples were tested at each temperature. In Phase 2, only the even-numbered samples were heat treated while the odd-numbered samples were as cast.

The peak sample stress levels were chosen to correspond with four fixed strains. The strains corresponded with four tip deflections, and the peak stresses were computed afterwards. Thus, the stress levels varied from material to material. In order to avoid hysteresis effects, all data were taken in increasing stress order from the lowest to highest stress.

Temperature tests were performed with the sample and "hinge" portion of the supporting structure enclosed in a temperature chamber. The accelerometer was changed from the BBN501 shown in Figure 3 to a B&K high temperature accelerometer for the 400° F tests. We encountered difficulties in thermal isolation of the heavy base from the "hinge" and sample during Phase 1, causing the 200° F tests there to have actually been run at sample temperatures of 217°-232° F. The problems were corrected before the 400° F tests were done in Phase 1, and before all of Phase 2. Tests were run on accelerometer sensitivity at the higher temperatures, and corrections were made to the observed levels.

2.3 Results

2.3.1 Phase 1 Results

The computed loss factors for the materials in Phase 1 are summarized in the first three Tables of Appendix C and in Figures 5-16. Included in the Tables are the measured natural frequencies, the computed Young's modulus, the peak sample stress, and the loss factor. An estimate of maximum air damping is included, from which corrected sample loss factors were calculated. The figures display the total measured damping (loss factor), including that due to the air.

The results will be discussed in groups, as there are similarities in the results for similar composites. The spread in data is shown in the figures, and the same symbols and line types always represent the same measurement temperatures. The abscissa also remains constant from figure to figure, but the ordinate may change.

Graphite Composites

In the first group (Figures 5-8), the graphite composites are shown. The graphite/aluminum composites show similar results in both magnitude and trend of loss factor with temperature. The materials exhibit higher losses at room temperature than at elevated temperature, and increasing loss factor with stress. Loss factors in graphite/aluminum composites range from .0025 to .0075 at room temperature, and .0004 to .005 at elevated temperature for 6-27.4 ksi peak sample stress. The graphite/ZE41A magnesium composites exhibit a temperature dependence similar to the graphite/aluminum composites. However, they generally exhibited lower loss factors at comparable temperatures, with loss factors ranging from .001 to .003 at room temperature and .0001 to .001 at elevated temperature (peak sample stresses of 5.4 to 23.5 ksi). The 100 Msi graphite/ZE41A magnesium composite showed slightly higher loss factors than the 55 Msi graphite/ ZE41A Mg composite.

FP Composites

In the next group (Figure 9-11) are 50 v/o FP composites with different matrix metals. The FP/aluminum composite exhibits higher loss factors than the FP/C.P. magnesium composite, which in turn exhibits greater damping than the FP/ZE41A magnesium composite. In the FP/Al composite, the loss factor decreases with increasing temperature, and increases with increasing peak sample stress. Values of loss factor range from 1.5 X 10^{-4} to .003 at peak sample stresses ranging from 7.8 to 29.6 ksi. The FP/Mg composites show a change in ordering of loss factor with temperature, with the highest loss factors occurring at room temperature. 400° F the intermediate, and 200° F the lowest. We believe this may be due to stress relief of the composite material. The loss factors in the FP/Mg composites range from 1.3 X 10^{-4} to .0014 at peak sample stresses ranging from 7.5 to 28.4 ksi.

SiC/Aluminum Composites

In the next group (Figures 12 and 13) are silicon carbide/ 6061 Aluminum composites, with the SiC in either whisker or particulate form. At room temperature, the loss factors of the two materials are very similar, while at elevated temperatures, the 45 v/o particular SiC composite exhibits less damping than the 20 v/o whisker SiC composite. The lowest losses occur at 200° F, and increase with increasing stress. The loss factors range from 2.5 to 8.3 X 10^{-4} at peak sample stresses between 3.9 and 26.6 ksi.

Unreinforced Base Metals

The final group (Figures 14-16) includes the base materials, 6061 Aluminum, ZE41A Magnesium, and Commercially Pure Magnesium. The measured loss factors in 6061 Al are much lower than those in the magnesium materials. All loss factors increase with increasing peak stress level. The magnesium materials show increasing loss factor with temperature, while in 6061 Aluminum, the measurements at room temperature are higher than the other two. The loss factors measured in commercially pure magnesium are, similarly, much higher than those in ZE41A Magnesium at the same stress levels. Loss factors in 6061 Al ranged from .0003 to .0014 at peak sample stresses between 4.1 and 26.7 ksi. In ZE41A Mg, loss factors were between .0005 to .006 at peak sample stresses ranging from 3.3 to 9 ksi. Loss factors in the commercially pure magnesium range from .0037 to 2.2 for peak sample stresses between 2.7 and 9.0 ksi. Each of the commercially pure magnesium samples exhibited fatigue and one broke (the one at which a loss factor, η, of 2.2 was measured).

Composite vs Base Metal Comparisons

A comparison of the results for the composite materials with those for the corresponding base metals reveals some interesting trends. The graphite/aluminum composites (Figures 5 & 6) have higher loss factors than unreinforced 6061 Aluminum (Figure 14), while those for the silicon carbide/aluminum composites (Figures 12 & 13) are comparable to or slightly lower than those for the base metal. The graphite/ZE41A Mg composites (Figures 7 & 8) have lower loss factors than unreinforced ZE41A Mg (Figure 15), as does the FP/ZE41A Mg composite (Figure 10). Similarly, the FP/CP Mg composite (Figure 11) has much lower loss factors than does the base metal (Figure 16). It is assumed that these results might be explained by the relative difference in magnitude of loss factors of the individual materials. Thus, the graphite fibers would have loss factors higher than 6061 Al, but lower than ZE41A Mg, while FP and SiC would have the lowest loss factor.

2.3.2 Phase 2 results

The computed loss factors for the materials in Phase 2 are summarized in the last six Tables of Appendix C and in Figures 17-24. Included in the Tables are the measured natural frequencies, computed Young's modulus, peak sample stress, and loss factor. An estimate of air damping is included, from which an average corrected sample loss factor is calculated. The Figures display the total measured damping (loss factor) in each sample, including that due to the air, linearly versus linear peak sample stress.

As the purpose of this phase was to assess the effects of heat treatment, fiber volume fraction (v/o), and fiber orientation on loss factor in FP/ZE41A Mg composites, these results will be discussed in turn. As in Phase 1, the spread in data is shown in the Figures and the same symbols and line types always represent the same measurement temperatures. The abscissa and ordinate are the same for all figures in this group.

Effects of Heat Treatment

A comparison of the results for as cast with those for heat treated (T-5) samples show that higher losses are achieved after heat treatment. This holds true regardless of volume fraction or fiber orientation (Figures 17 versus 18, 19 versus 20, 21 versus 22, or 23 versus 24). Sample to sample variations can be observed. The effect of heat treatment, while consistent, is generally not large where loss factor is roughly linearly increasing with stress. Larger effects are seen in the samples with $\pm 22\frac{1}{2}^{\circ}$ fiber orientation.

Effects of Fiber Volume Fraction (v/o)

A similar comparison between the loss factors in 35 v/o samples with those of 56 v/o samples (Figures 17-20 versus Figures 21-24) shows that higher losses are achieved at lower fiber volume fraction. This result is consistent with one observed in Phase 1, that the composite loss factor is a combination of the loss factors of the two components. The effect is somewhat more marked here, but the largest changes are again seen in the samples with $\pm 22\frac{1}{2}^{\circ}$ fiber orientation. A quick review of the data from Phase 1 (50 v/o) with these data (Figure 10 versus Figures 17 & 21) shows a similar trend, but the 400° F data are all nearly the same. No attempt is made to propose a theory of how the composite loss factor is determined from the loss factors of the two components.

Effects of Fiber Orientation

The effects of fiber orientation on loss factor are more pronounced than are the effects of the previous two parameters. In this case, we compare Figure 17 versus 19, 18 versus 20, 21 versus 23, and 22 versus 24. The observed loss factors are much higher for samples with $\pm 22\frac{1}{2}^{\circ}$ fiber orientation when compared with 0° orientation. Further, the behavior of loss factor with peak sample stress is different in the two cases: for 0° orientation, the loss factor is increasing approximately linearly with stress, while for $\pm 22\frac{1}{2}^{\circ}$ orientation, the loss factor increases almost exponentially with stress. In the $\pm 22\frac{1}{2}^{\circ}$ samples, this increase in loss factor with stress becomes more rapid with increasing temperature.

Experimental error in Phase 2 was not generally large, but sample-to-sample differences frequently were. Errors due to air damping could be important, if the application does not encounter amplitudes of vibration similar to those in this experiment. Air damping estimates had the most impact at room temperature and at 400° F. For details, the reader is referred to Appendix C.

Measured loss factors in Phase 2 ranged from 2×10^{-4} at 400° F to 3.8×10^{-3} at room temperature. Greatest variations (of all kinds) occurred in the $\pm 22\frac{1}{2}^{\circ}$ samples. Peak sample stresses ranged from 4.6 to 29.3 ksi and resonant frequencies were between 125.4 and 149.1 Hz at the lowest stress at room temperature.

2.4 Summary

Resonant dwell damping tests were run on nine different metal matrix composites, three base metals, and eight configurations of FP/ZE41A Mg. The samples, cantilever beams, were tested at their fundamental frequency, between 100 and 200 Hz. Tests were run at three temperatures and four peak sample stress levels below 30,000 psi. In general, the loss factor increased or remained the same with increasing peak sample stress level for all materials tested.

Analysis of the loss factor data for the two Phases in this study revealed several things. In Phase 1, it was noted that only the graphite/aluminum composites had higher loss factors than the base metal; all other composite materials exhibited lower or comparable loss factor when compared with the corresponding base metal. For the graphite composites, loss factors were highest at room temperature, and lower at the higher temperatures. Conversely, for the SiC reinforced or Magnesium base composites, loss factors were highest at 400° F. There was little other significant variation in loss factor with temperature. In Phase 2, it was determined that higher loss factors were achieved for samples heat treated to a T-5 condition, with 35 v/o FP, and with fiber orientations of $\pm 22\frac{1}{2}^{\circ}$ as compared with those as cast, with 50 or 56 v/o FP, and with fiber orientations of 0°, respectively. No general conclusions could be drawn about the dependence of loss factor on temperature.

3. RECOMMENDATIONS

As noted in the sections on results, it appears that the sample loss factor is a function of the relative amounts of the materials in the composite. We recommend that a study be done to develop a model which can predict the loss factor of a composite material based on its components. Such a theory would be especially useful in the development of higher loss structural materials.

The results in Phase 2 indicated that higher loss was achieved for a fiber orientation of $\pm 22\frac{1}{2}^{\circ}$ than was for 0°. We recommend that a study be done of how the loss factor of a FP/ZE41A Mg composite varies with fiber orientation. We also recommend that this study investigate theories that might explain the experimental results.

Finally, in view of the large sample-to-sample variations in properties of nominally the same composite, we recommend that a study be done to determine how ultrasonic or vibration test measurements can be applied to the quality control of the composite materials. The development of such a test procedure could be extremely important from a manufacturing standpoint.

REFERENCES

1. Timmerman, N. S., "Damping Characteristics of Metal Matrix Composites," BBN Report No. 4864, AMMRC TR82-19, April 1982

2. Granick, N. & Stern, J. E., "Material Damping of Aluminum by a Resonant - Dwell Technique," NASA TN D-2893 (1965)

3. Heine, J. C. "The Stress and Frequency Dependence of Material Damping in Some Engineering Alloys," Ph.D. Thesis, MIT (1966)

4. Grau, Frederick Earl Jr., "Air Damping of Vibrating Beams," S. M. Thesis, MIT (1966)

5. Plunkett, R., and Sax, M., "Nonlinear Material Damping for Nonsinusoidal Strain," Journal of Applied Mechanics, Vol. 45, No. 4, (1978)

6. Gibson, R. F., Yau, A., and Riegner, D. A., "An Improved Forced-Vibration Technique for Measurement of Material Damping," Experimental Techniques, Vol 6., No. 2, (1982)

7. Heine, J. C. "Air Damping of Vibrating Cantilever Reeds," Quarterly R&D Progress Report No. 321Y 08 05, MIT A & V Laboratory, June, 1964.

8. Harris and Crede, *Handbook of Sound and Vibration*, Second Ed., McGraw-Hill Book Co., New York, 1976.

TABLE 1

PHASE 1 MATERIAL PROPERTIES

NO.	FIBER	BASE METAL	VOLUME FRACTION FIBER (%)	MATERIAL DENSITY (lb_m/in^3) QUOTED	MATERIAL DENSITY (lb_m/in^3) MEASURED**	YOUNG'S MODULUS (10^6psi) QUOTED	YOUNG'S MODULUS (10^6psi) MEASURED*
1	55 Msi Graphite	6061 Aluminum	50	.085	.085	26.43 ± .95	23 - 25
2	100 Msi Graphite	6061 Aluminum	50	.085	.086	42.5 ± 2.7	39.5 - 41.5
3	55 Msi Graphite	ZE41A Magnesium	50	.068	.069	23.14 ± .93	21 - 24
4	100 Msi Graphite	ZE41A Magnesium	50	.068	.071	40.75 ± .4	33 - 35.5
5	FP (Al_2O_3)	2% Li Aluminum	50	.1156	.116	32	30 - 32
6	FP (Al_2O_3)	ZE41A Magnesium	50	.1048	.102	30	29.5 - 30
7	FP (Al_2O_3)	Comm. Pure Magnesium	50	.1043	.104	30	29.5 - 30.1
8	Particulate SiC	6061 Aluminum	45	.104	.106	21.95 ± .71	20 - 22.5
9	Whisker SiC	6061 Aluminum	20	.102	.102	14.09 ± .62	14 - 16
AL	--	6061 Aluminum	0	.0975	.097	10.6	8 - 10
RZ	--	ZE41A Magnesium	0	.066	.066	7.4	6.5 - 7.3
CP	--	Comm. Pure Magnesium	0	.063	.062	6.5	5.3 - 6.1

**Density values measured with accuracy estimated at ± 1 percent.

*Values at lowest stress level inferred from natural frequency.

TABLE 2

PHASE 2 COMPOSITE MATERIAL PROPERTIES
FP(Al_2O_3)/ZE41A MAGNESIUM SAMPLES

DESIGNATION	BATCH	FIBER VOLUME FRACTION (%)	FIBER ORIENTATION	HEAT TREATMENT	LONG. TENSILE STRENGTH (ksi)	DENSITY (g/cm^3) QUOTED	DENSITY (g/cm^3) MEASURED**	YOUNG'S MODULUS (10^6psi) QUOTED	YOUNG'S MODULUS (10^6psi) MEASURED*
A-odd	263GP-3	35	$\pm 0^o$	As Cast	44.2 - 49.8	2.46	2.45 - 9	21 - 23	22 - 25
A-even	263GP-3	35	$\pm 0^o$	T-5	53.1	2.46	2.44 - 9	N/A	21.4 - 23.5
B-odd	263GP-31	35	$\pm 22\frac{1}{2}^o$	As Cast	40.7 - 41.0	2.56	2.51 - 4	18 - 21	17.8 - 18.6
B-even	263GP-31	35	$\pm 22\frac{1}{2}^o$	T-5	41.4	2.56	2.52 - 4	N/A	17.9 - 19.2
C-odd	263GP-33	35	$\pm 22\frac{1}{2}^o$	As Cast	47.7 - 48.5	2.58	2.54	18 - 21	19.5
C-even	263GP-33	35	$\pm 22\frac{1}{2}^o$	T-5	50.0	2.58	2.55	N/A	18.8
D-odd	254GP-4	56	$\pm 0^o$	As Cast	70.8 - 77.2	2.94	2.84 - 9	28 - 30	27.8 - 29.4
D-even	254GP-4	56	$\pm 0^o$	T-5	68.8	2.94	2.86 - 8	N/A	27.8 - 29.5
E/J-odd	256GP-7	56	$\pm 22\frac{1}{2}^o$	As Cast	53.1 - 62.5	2.93	2.87 - 90	25 - 28	24.8 - 26
E/J-even	256GP-7	56	$\pm 22\frac{1}{2}^o$	T-5	63.0	2.93	2.85 - 9	N/A	25.4 - 25.8
F-odd	250GP-14	56	$\pm 22\frac{1}{2}^o$	As Cast	56.1	2.95	2.88 - 90	25 - 28	25.8 - 27.7
F-even	250GP-14	56	$\pm 22\frac{1}{2}^o$	T-5	51.6	2.95	2.88 - 9	N/A	25.2 - 25.6

**Density values measured with accuracy estimated at ± 1 percent.

N/A = Not Available

*Values at lowest stress level inferred from natural frequency.

TABLE 3

Temperature Distribution of Sample Numbers

Material Designation		Room Temperature	200° F	400° F
Phase 1:	1-	1	2	3
	2-	1	2	3
	3-	1	2	3
	4-	1	2	3
	5-	1	2	3
	6-	1	2	3
	7-	1	2	3
	8-	1	2	3
	9-	1	2	3
	AL-	1	2	3
	RZ-	1	2	3
	CP-	1,3	2	3
Phase 2:				
As Cast:	A-	1,7	3,9	5,11
	B-	1	3,7	5,9
	C-	1		
	D-	1,7	3,9	5,11
	E/J-	3	5	1,7
	F-	1	3	
Heat Treated (T-5):	A-	2,8	4,10	6,12
	B-	4	2,8	6,10
	C-	2		
	D-	2,8	4,10	6,12
	E/J-	4	6	2,8
	F-	2	4	

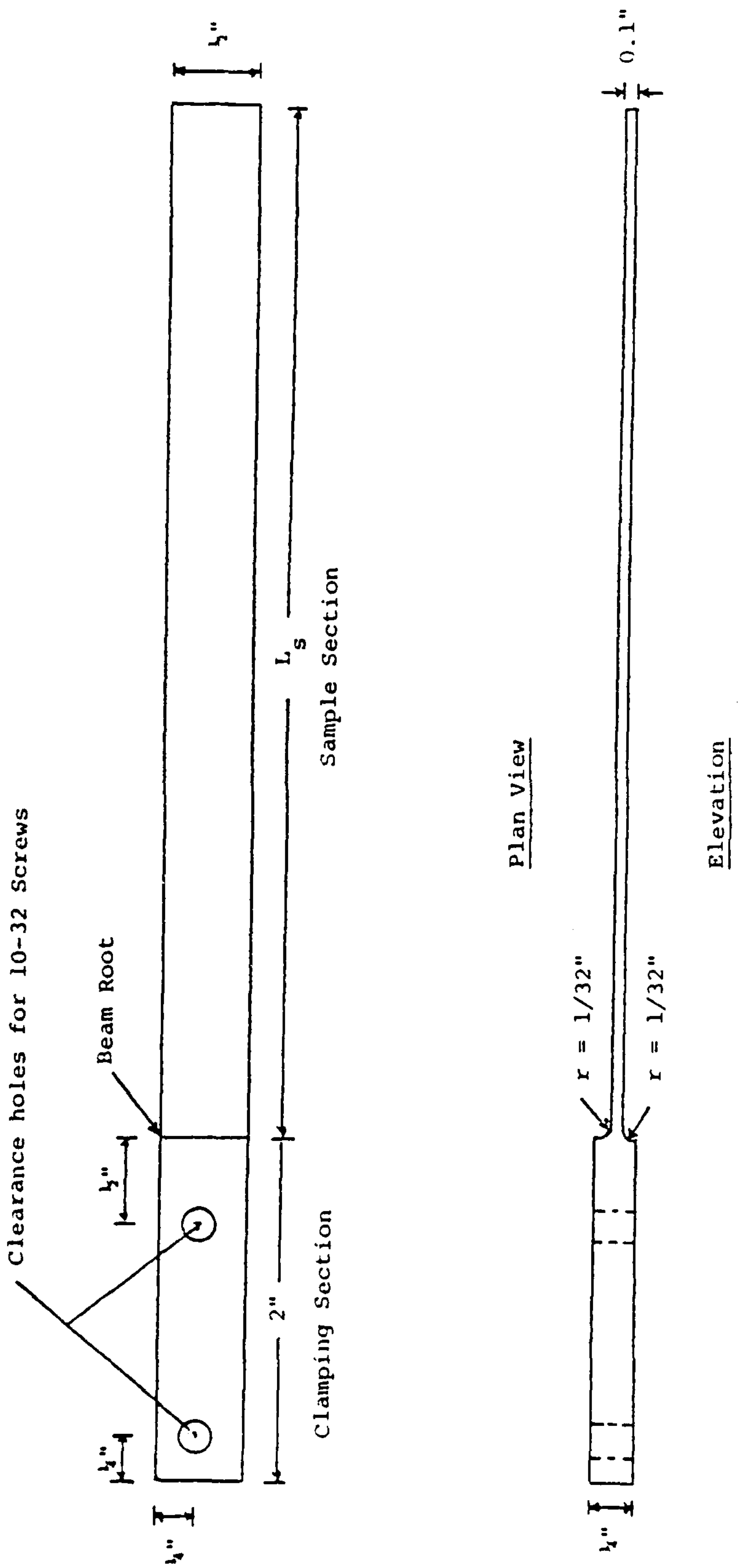

Tolerances: Clamping Section - ± .02"
Sample Section - ± .005"

FIGURE 1 METAL MATRIX COMPOSITE SAMPLE DIMENSIONS

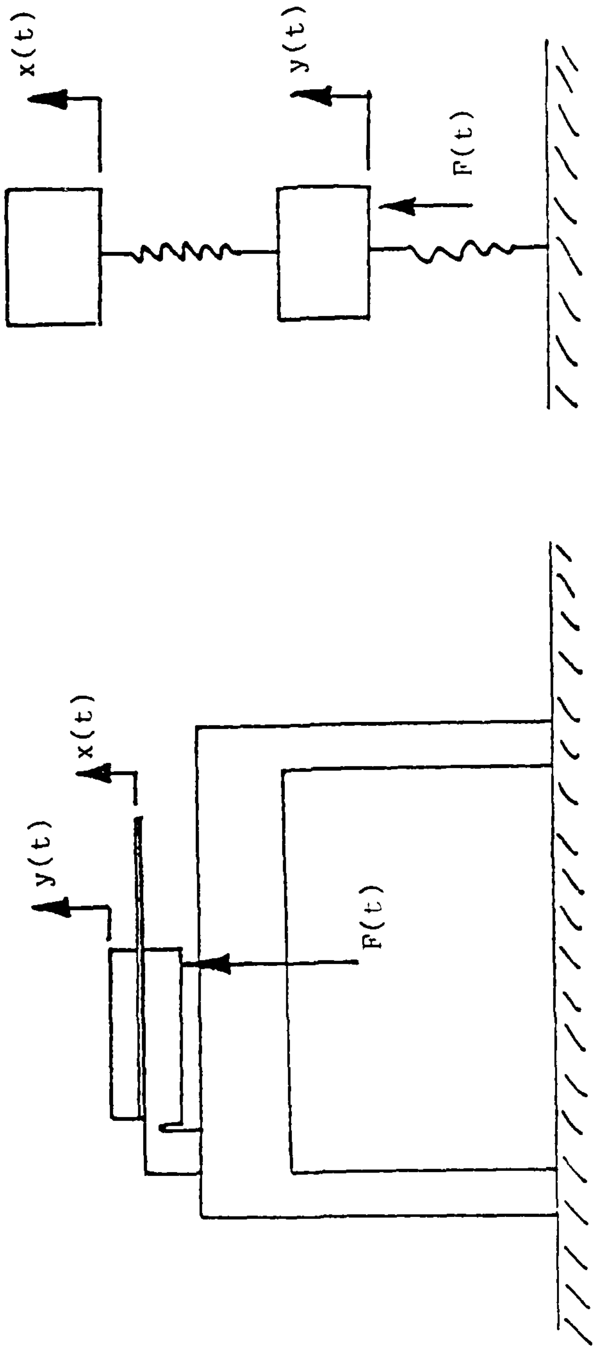

FIGURE 2

THE RESONANT DWELL DAMPING APPARATUS
IS THE EQUIVALENT OF AN EXCITED SYSTEM
WITH A RESONANT VIBRATION ABSORBER

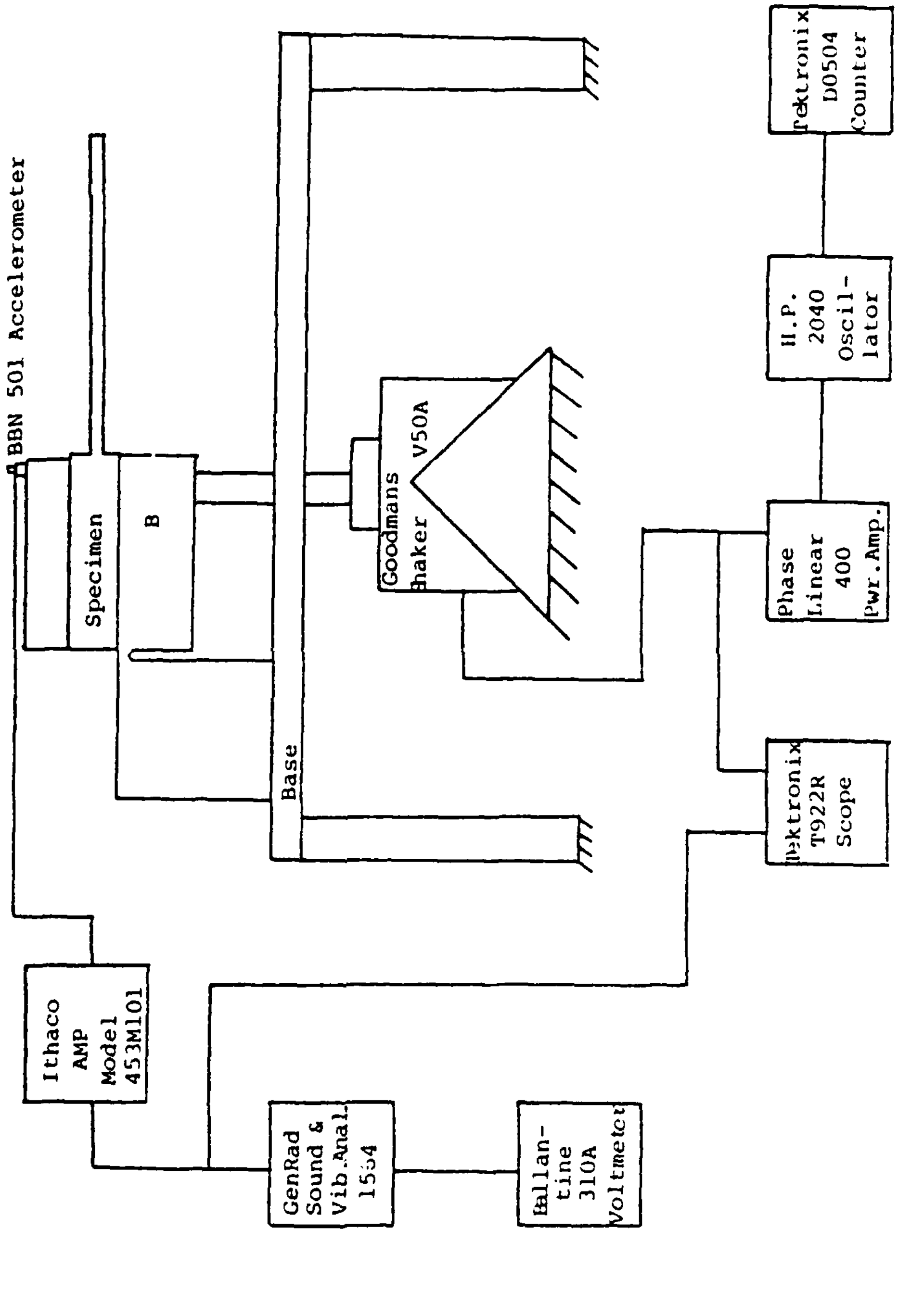

FIGURE 3. EXPERIMENTAL ARRANGEMENT FOR RESONANT DWELL TESTS

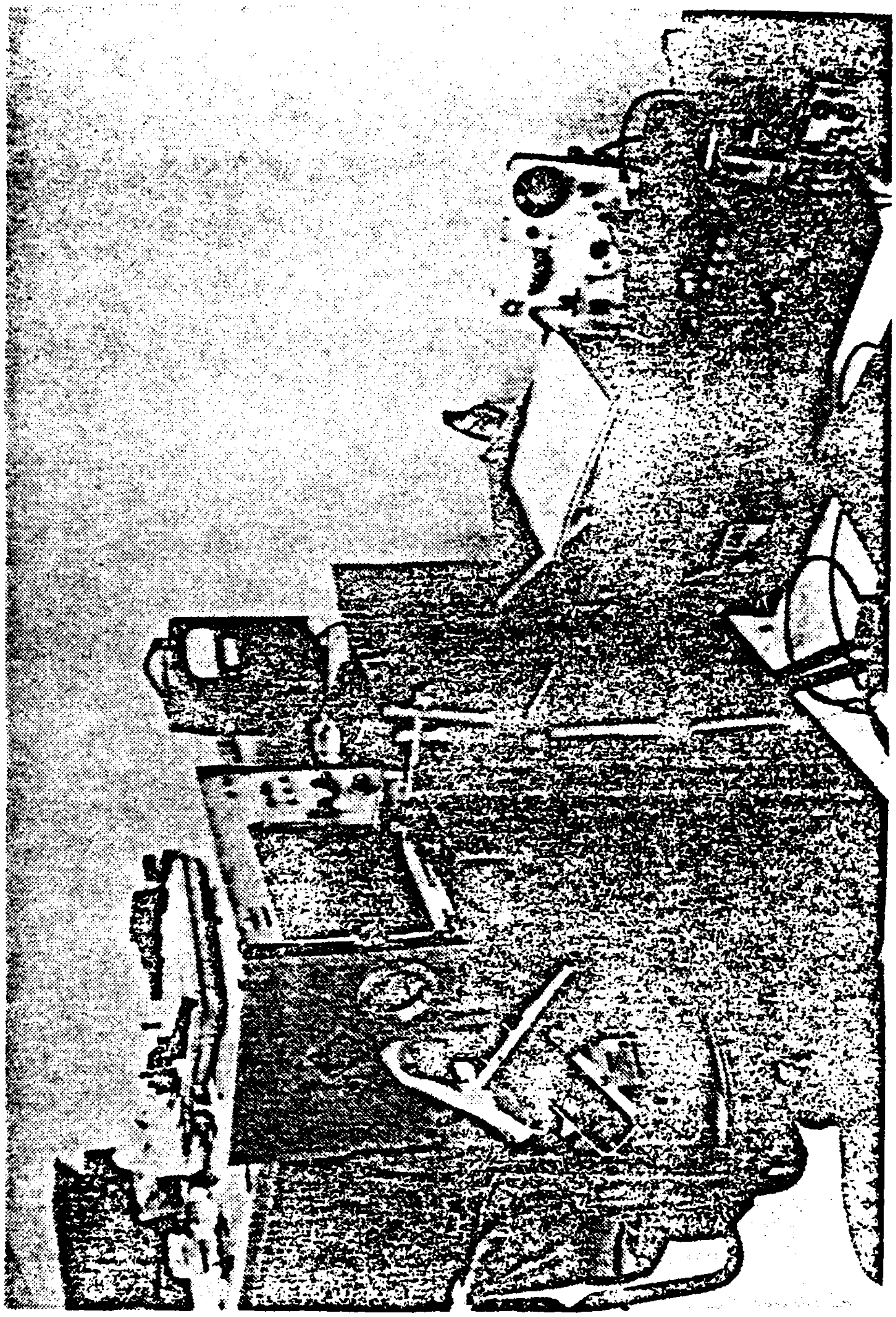

FIGURE 4. RESONANT DWELL TEST APPARATUS

EFFECTS OF STRESS AND TEMPERATURE
55 MSI GRAPHITE
6061 ALUMINUM

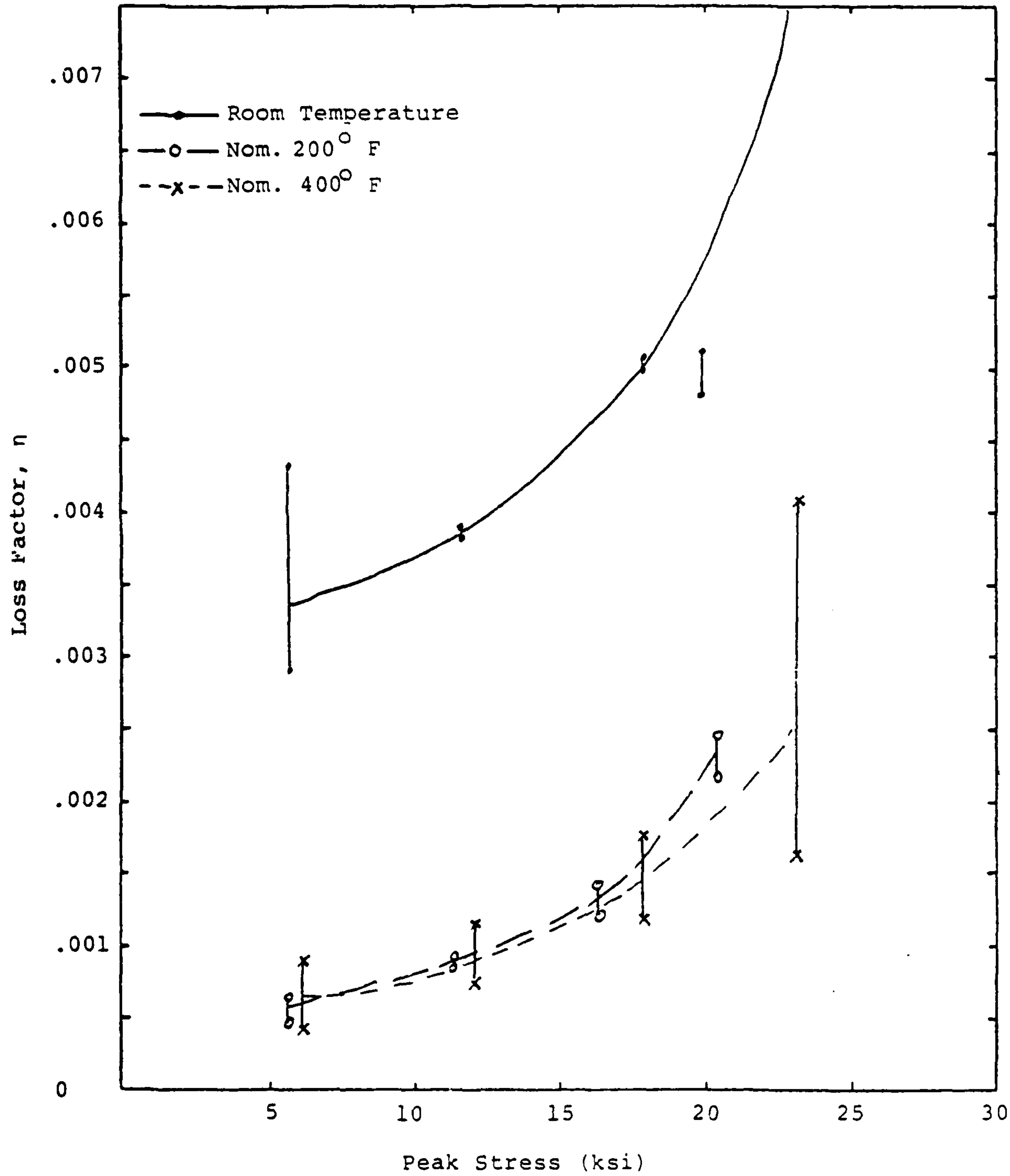

Figure 5

EFFECTS OF STRESS AND TEMPERATURE
100 Msi Graphite/
6061 Aluminum

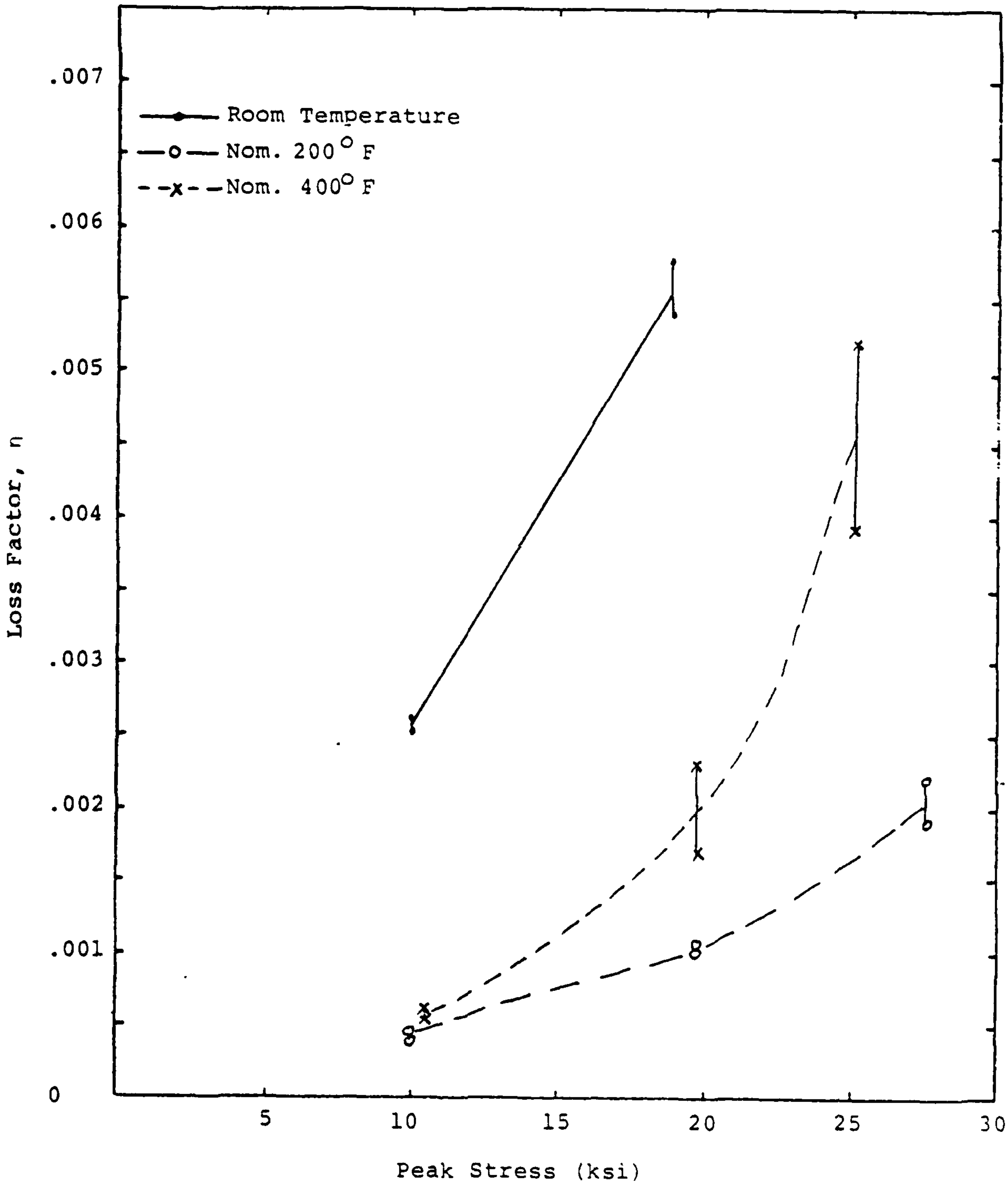

Figure 6

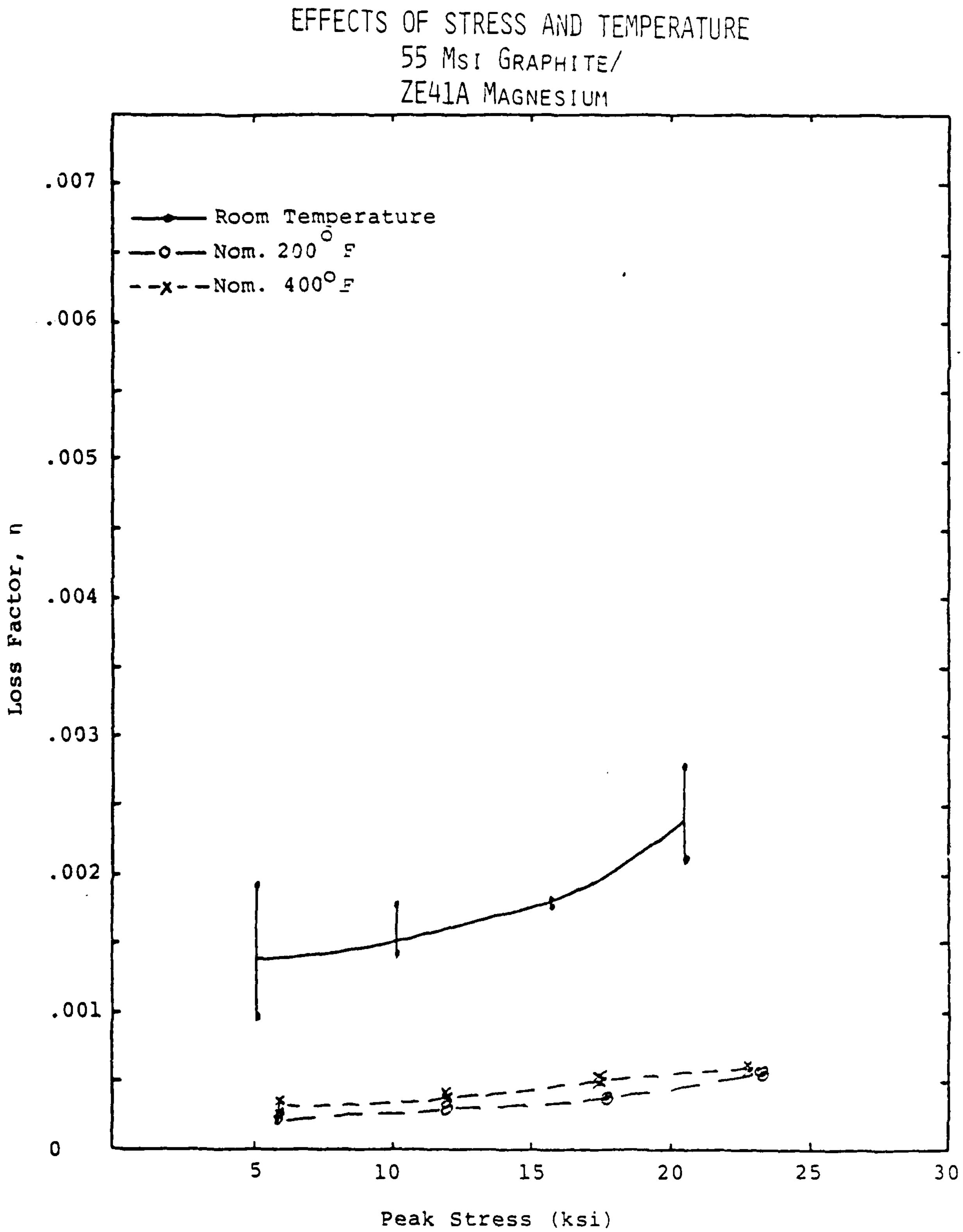
EFFECTS OF STRESS AND TEMPERATURE
55 Msi Graphite/
ZE41A Magnesium
Room Temperature
Nom. 200° F
Nom. 400° F
Loss Factor, η
.007
.006
.005
.004
.003
.002
.001
0
5
10
15
20
25
30
Peak Stress (ksi)

Figure 7

EFFECTS OF STRESS AND TEMPERATURE
100 MSI GRAPHITE/
ZE41A MAGNESIUM

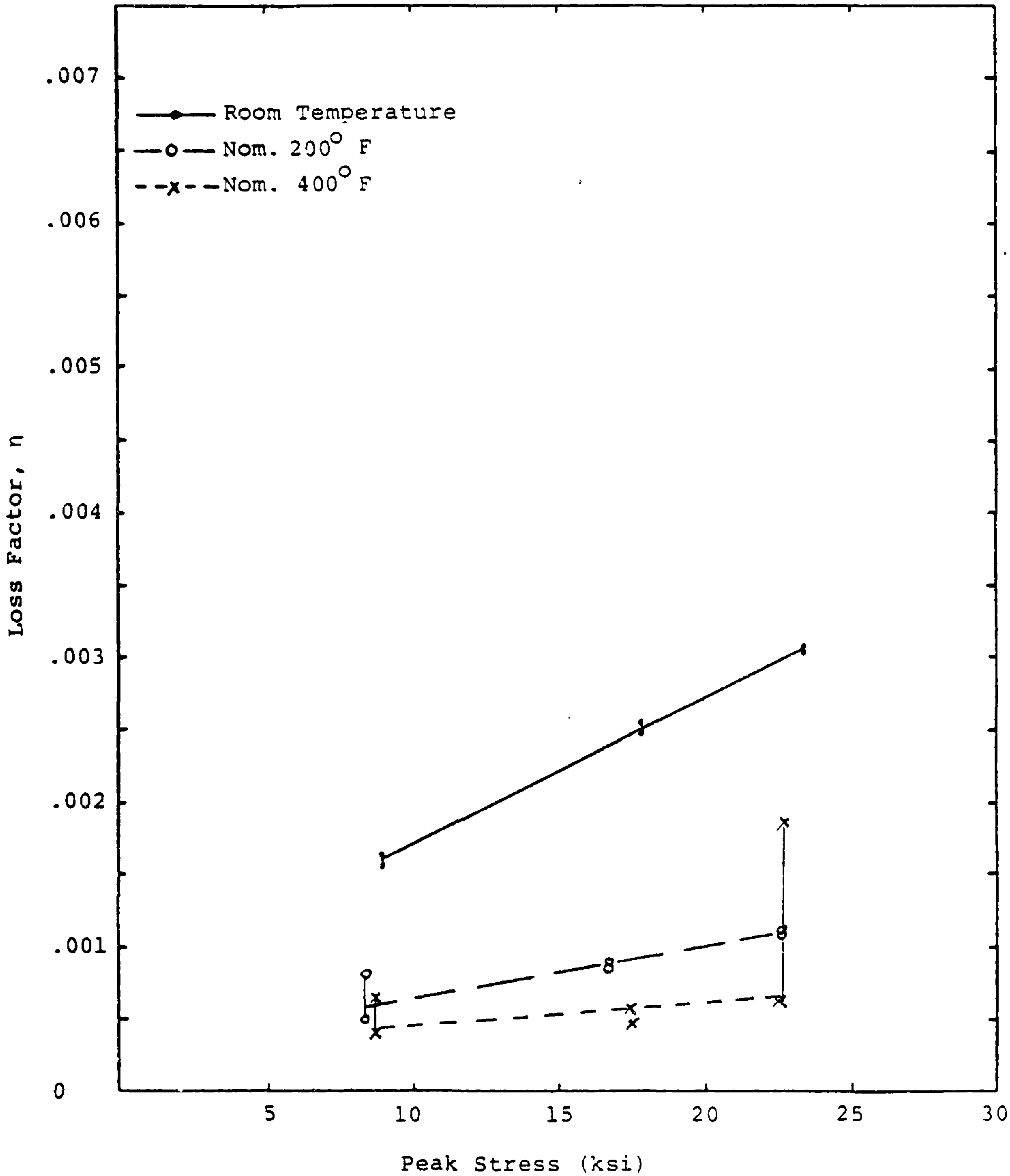

Figure 8

EFFECTS OF STRESS AND TEMPERATURE
FP/2% LITHIUM - ALUMINUM

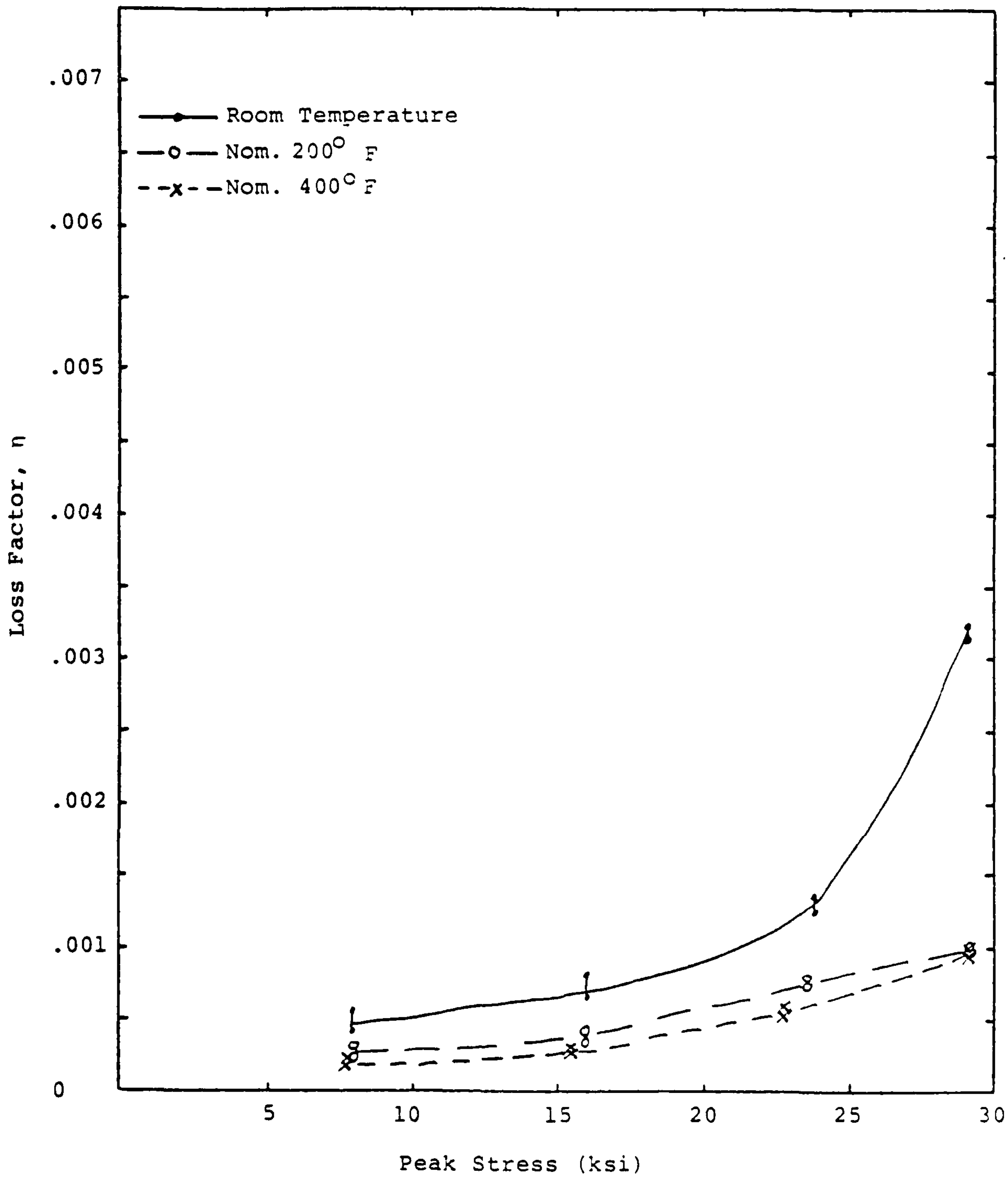

Figure 9

EFFECTS OF STRESS AND TEMPERATURE
FP/ZE41A Mg (50% v/o)

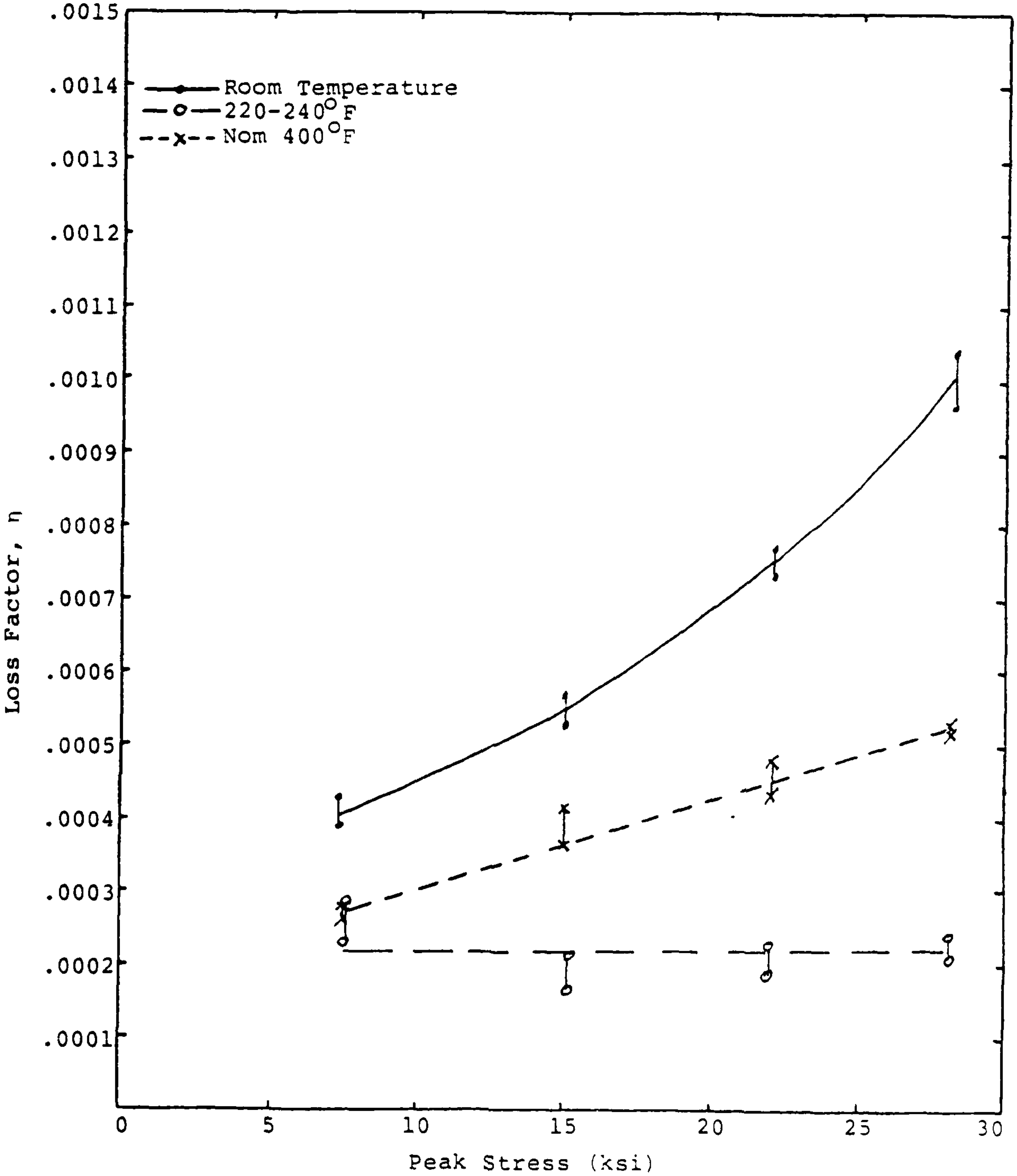

Figure 10

EFFECTS OF STRESS AND TEMPERATURE
FP/C.P. Mg (50% v/o)

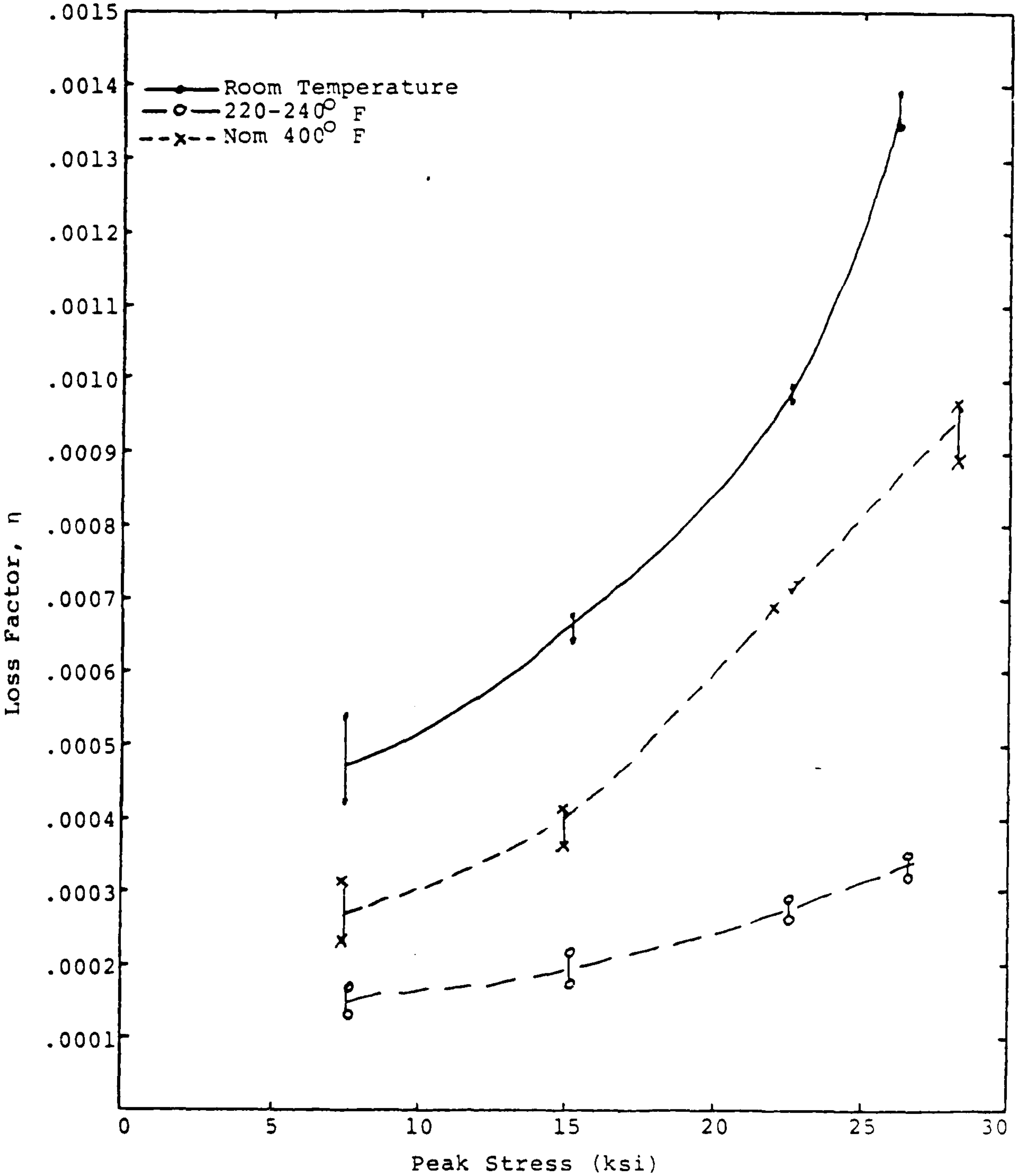

Figure 11

EFFECTS OF STRESS AND TEMPERATURE
SiC/6061 Al (45% Part.)

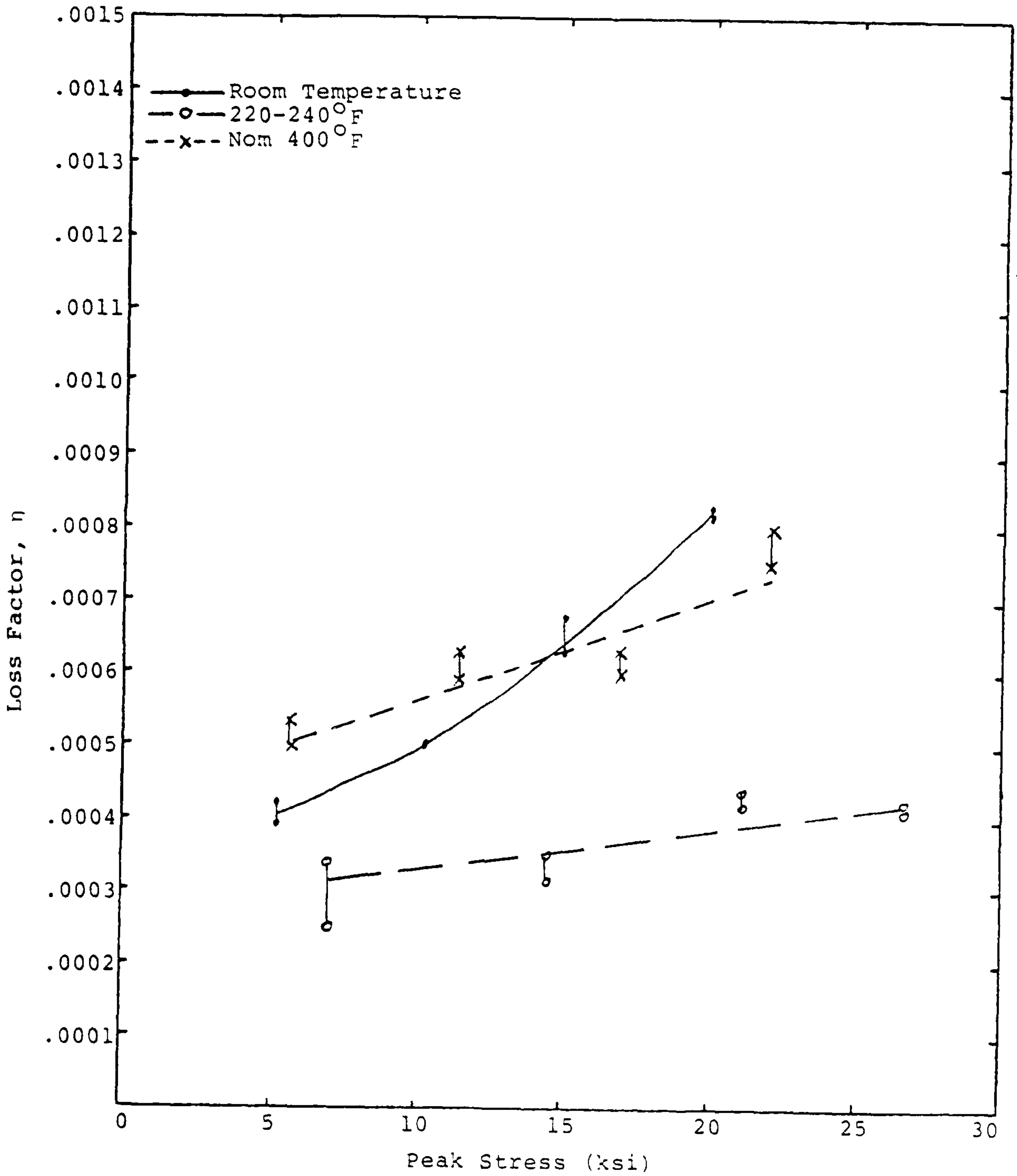

Figure 12

EFFECTS OF STRESS AND TEMPERATURE
SiC/6061 Al (20% wh.)

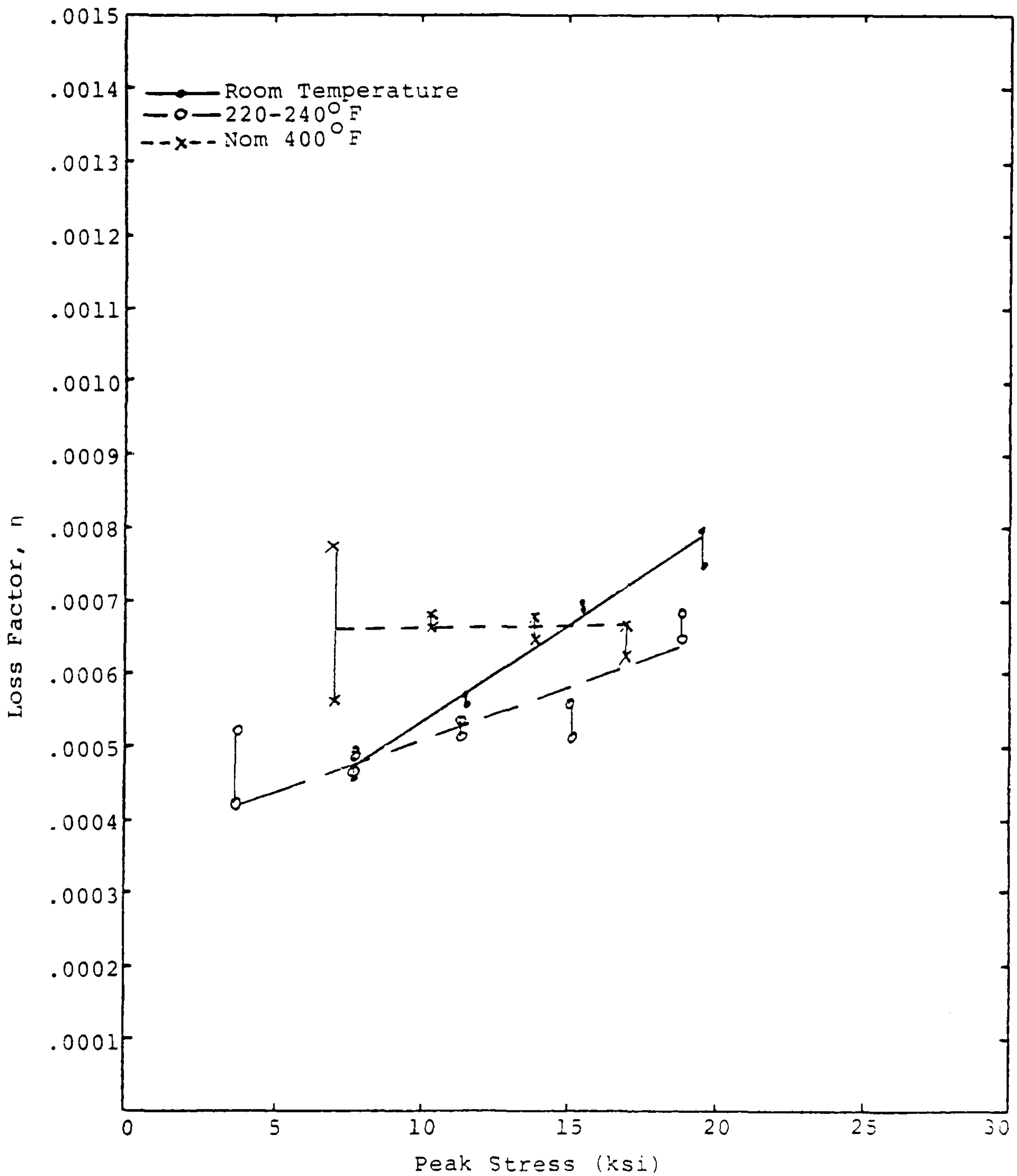

Figure 13

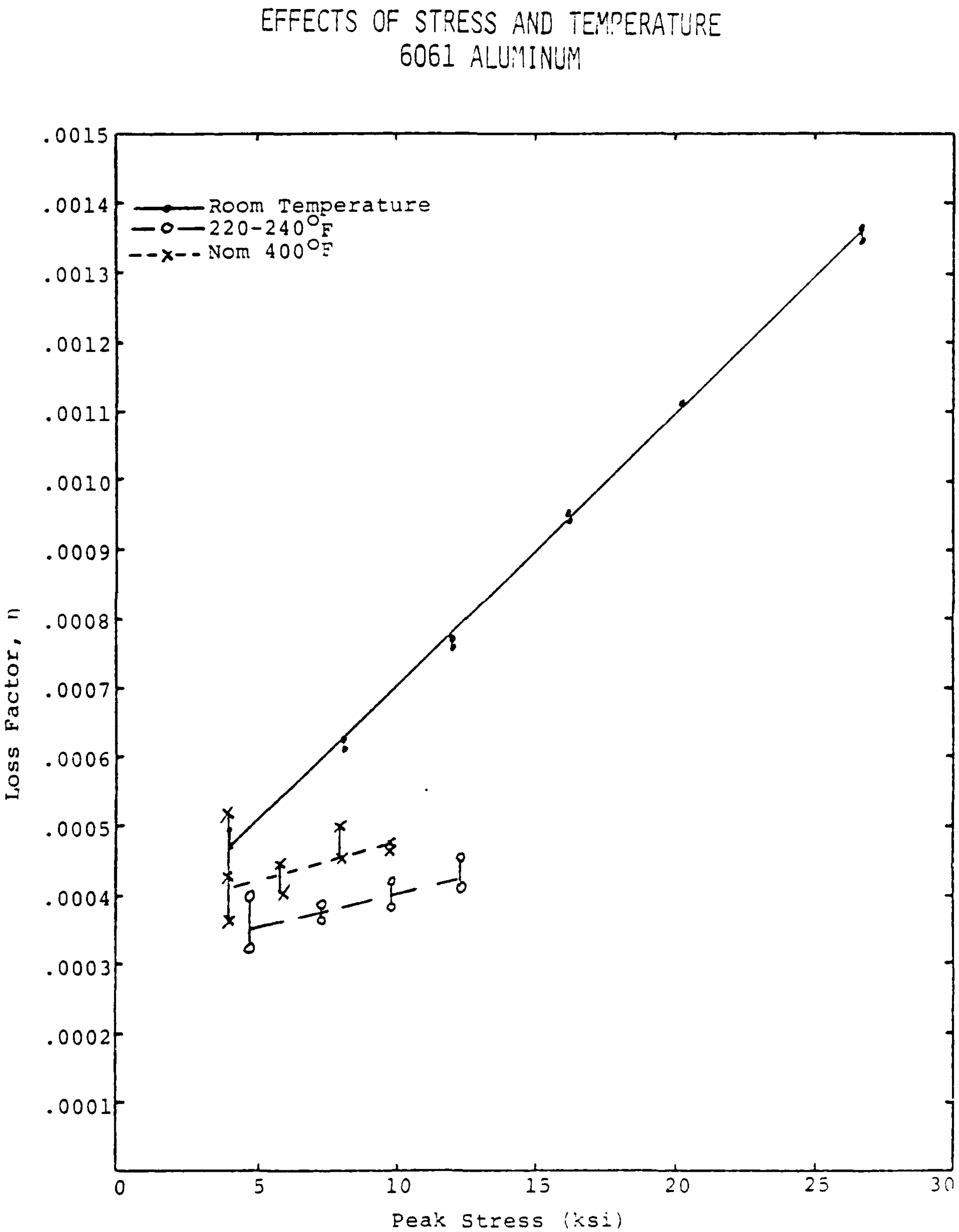

EFFECTS OF STRESS AND TEMPERATURE
6061 ALUMINUM
Room Temperature
220-240°F
Nom 400°F
Loss Factor, η
.0015
.0014
.0013
.0012
.0011
.0010
.0009
.0008
.0007
.0006
.0005
.0004
.0003
.0002
.0001
0
5
10
15
20
25
30
Peak Stress (ksi)

Figure 14

EFFECTS OF STRESS AND TEMPERATURE
ZE41A MAGNESIUM

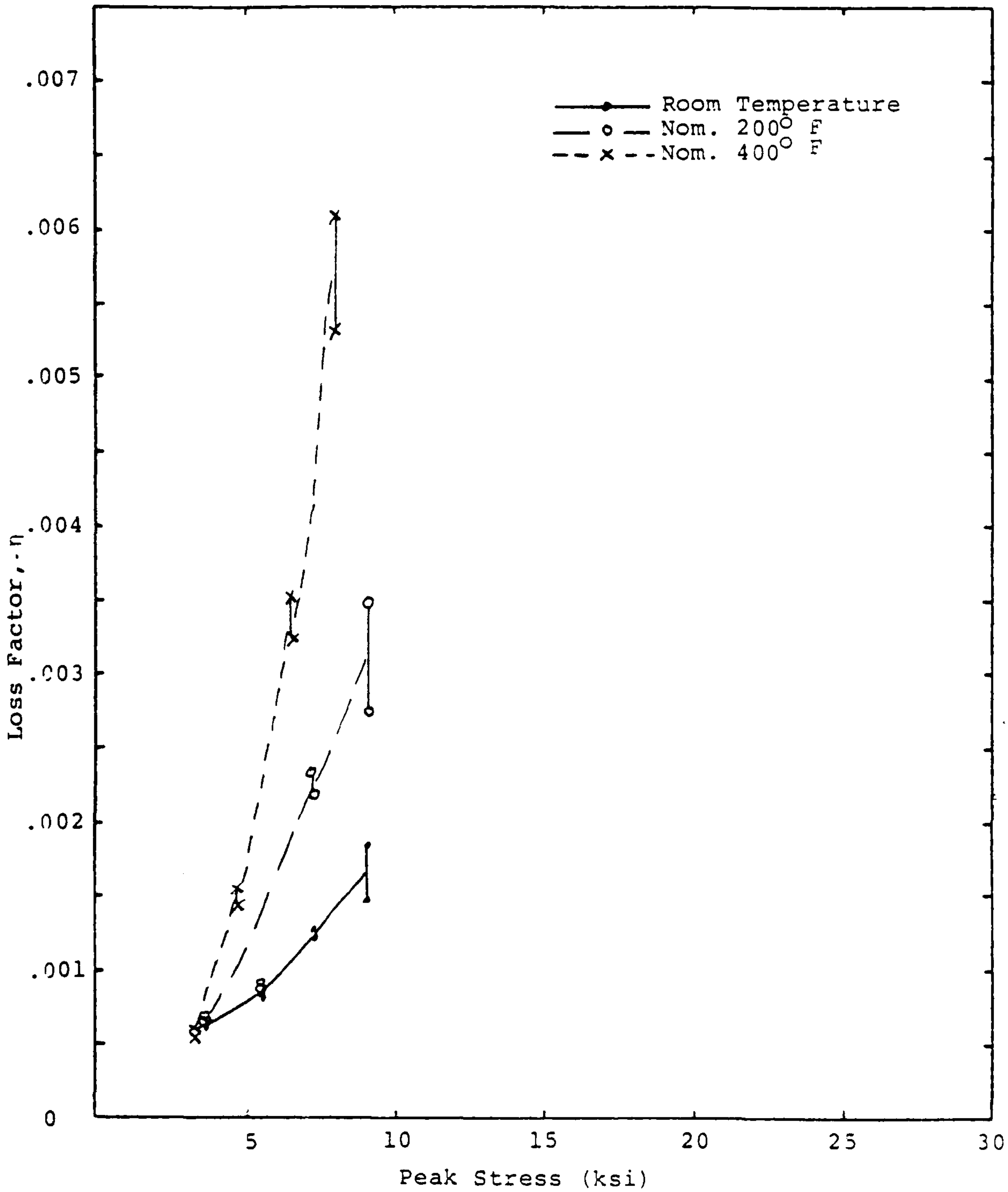

Figure 1?

EFFECTS OF STRESS AND TEMPERATURE
COMMERCIALLY PURE MAGNESIUM

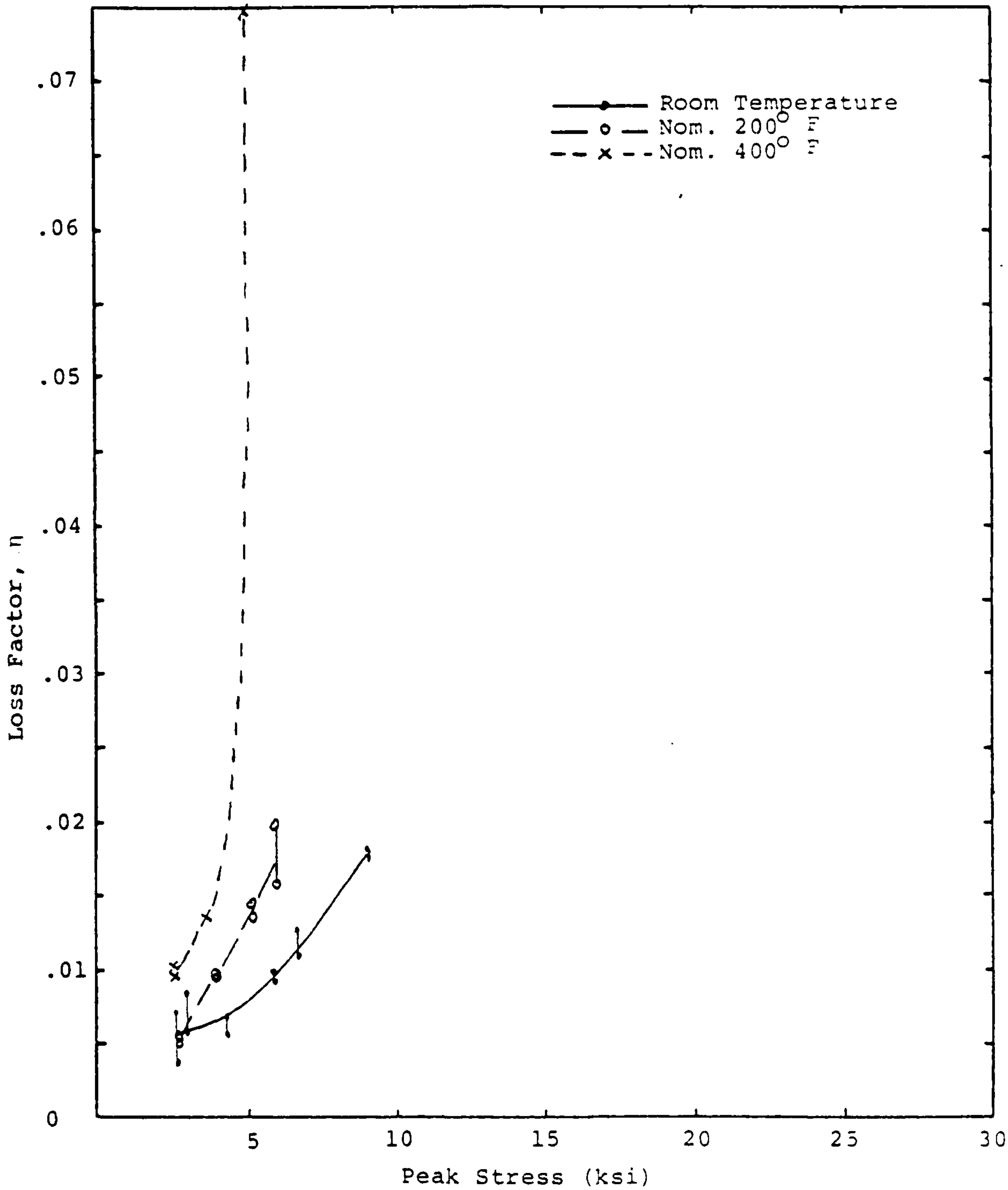

Figure 16

EFFECTS OF STRESS AND TEMPERATURE
$FP(Al_2O_3)$/ZE41A MAGNESIUM
35 v/o FP, 0^o FIBER ORIENTATION, AS CAST

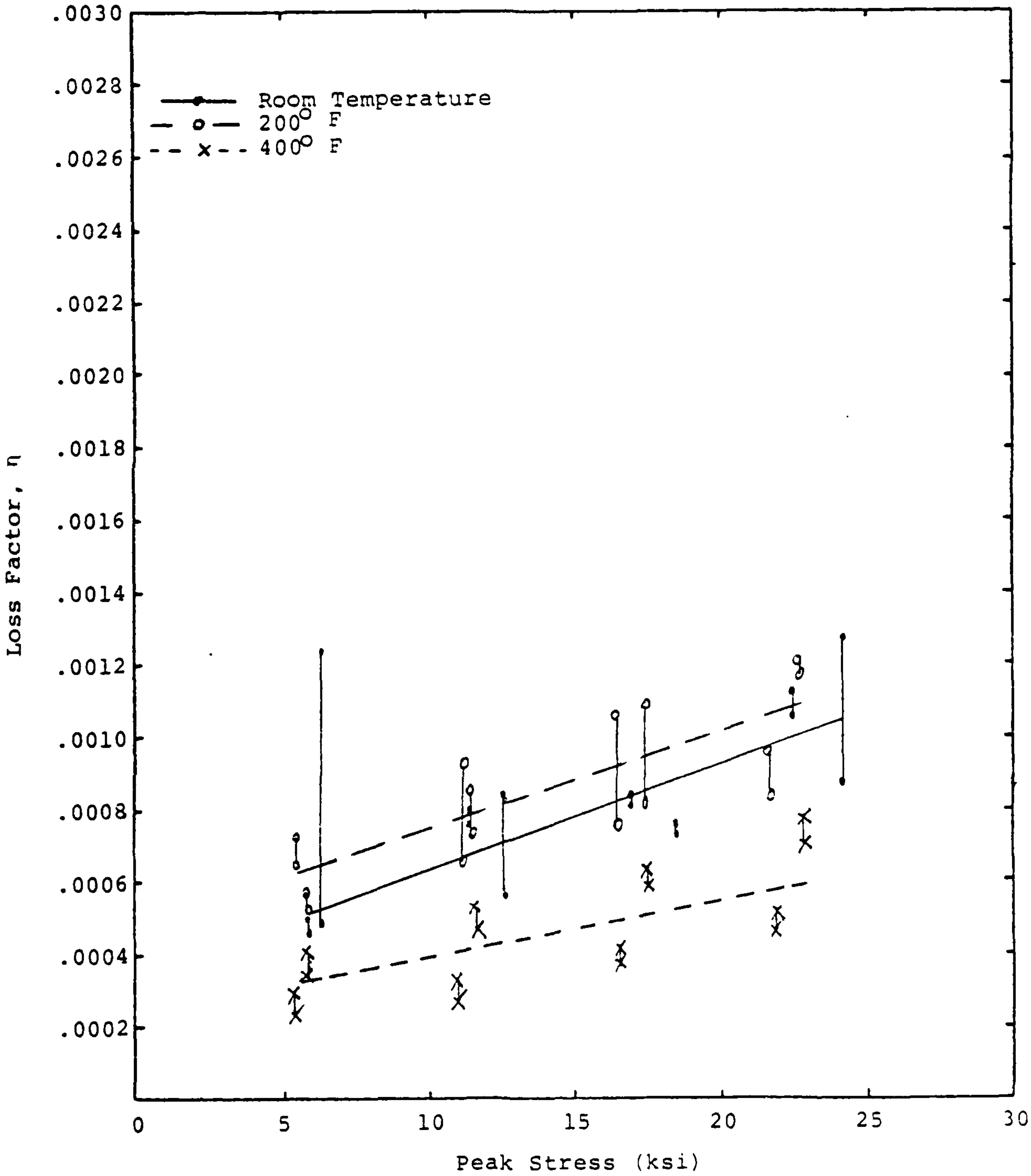

Figure 17

EFFECTS OF STRESS AND TEMPERATURE

$FP(Al_2O_3)/ZE41A$ MAGNESIUM

35 v/o FP, 0^{o} FIBER ORIENTATION, T-5 HEAT TREATED

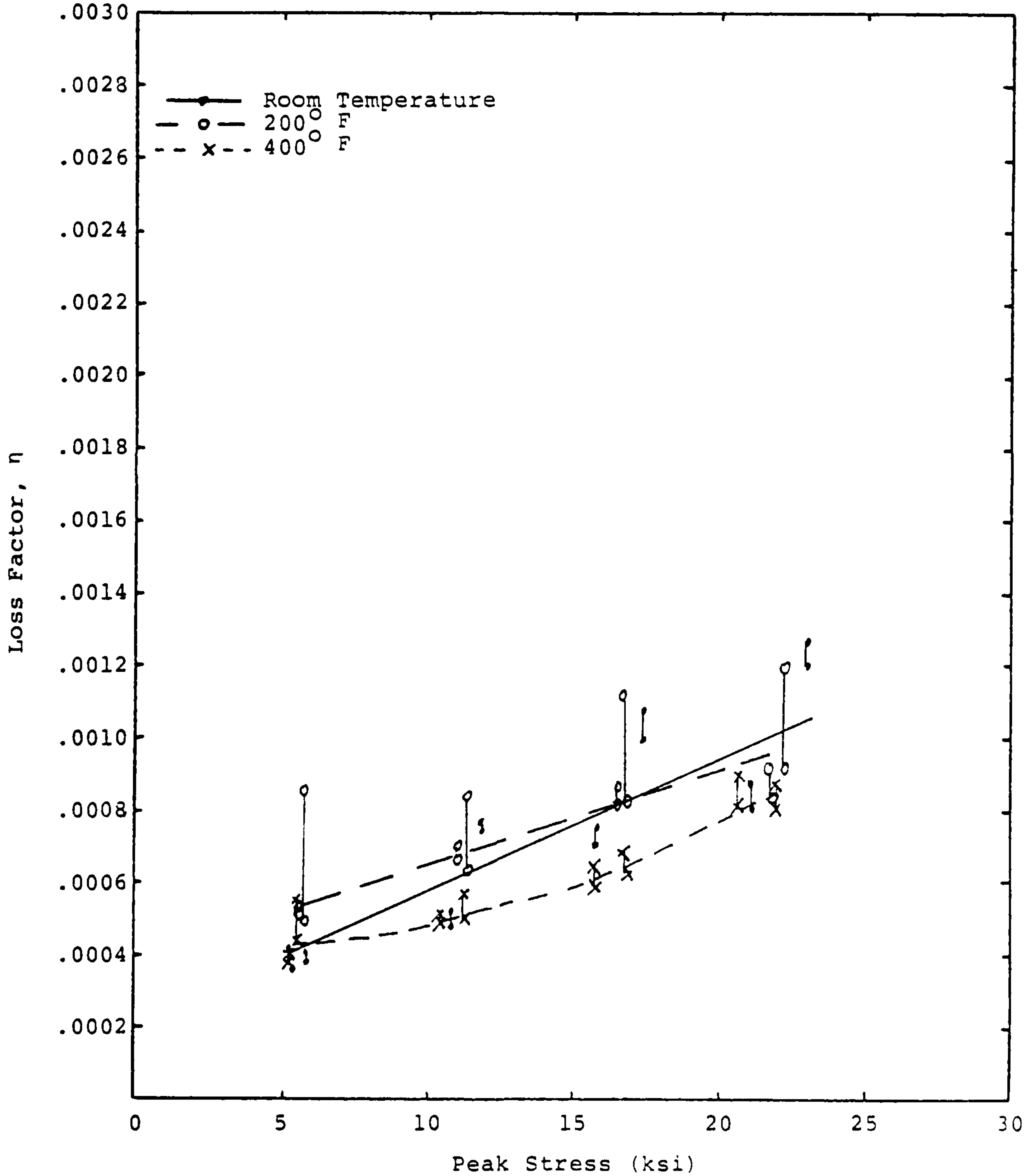

Figure 18

EFFECTS OF STRESS AND TEMPERATURE
FP(Al_2O_3)/ZE41A MAGNESIUM
35 v/o, ±22½ FIBER ORIENTATION, AS CAST

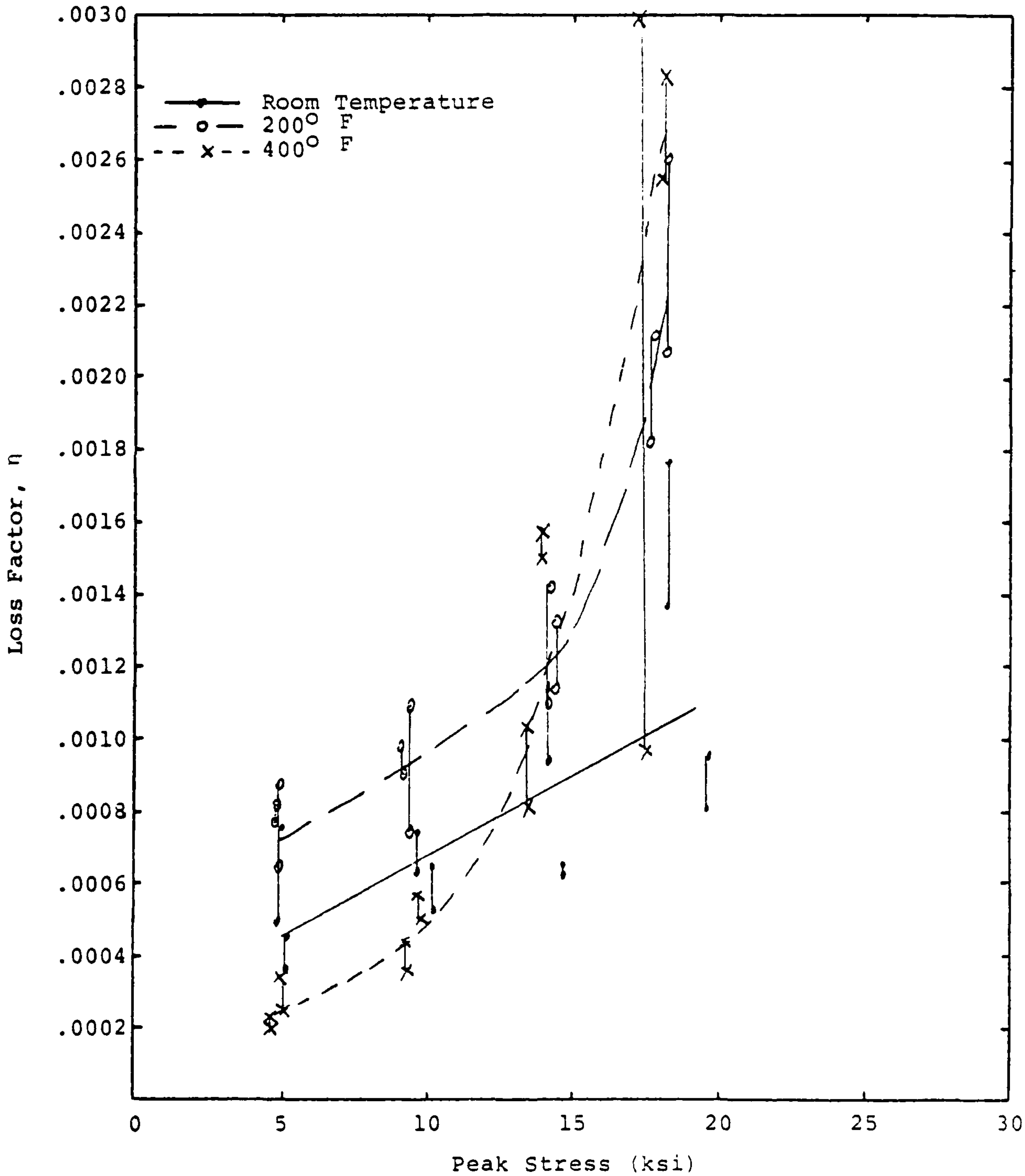

Figure 19

EFFECTS OF STRESS AND TEMPERATURE
FP(Al_2O_3)/ZE41A MAGNESIUM
35 v/o, ±22½° FIBER ORIENTATION, T-5 HEAT TREATED

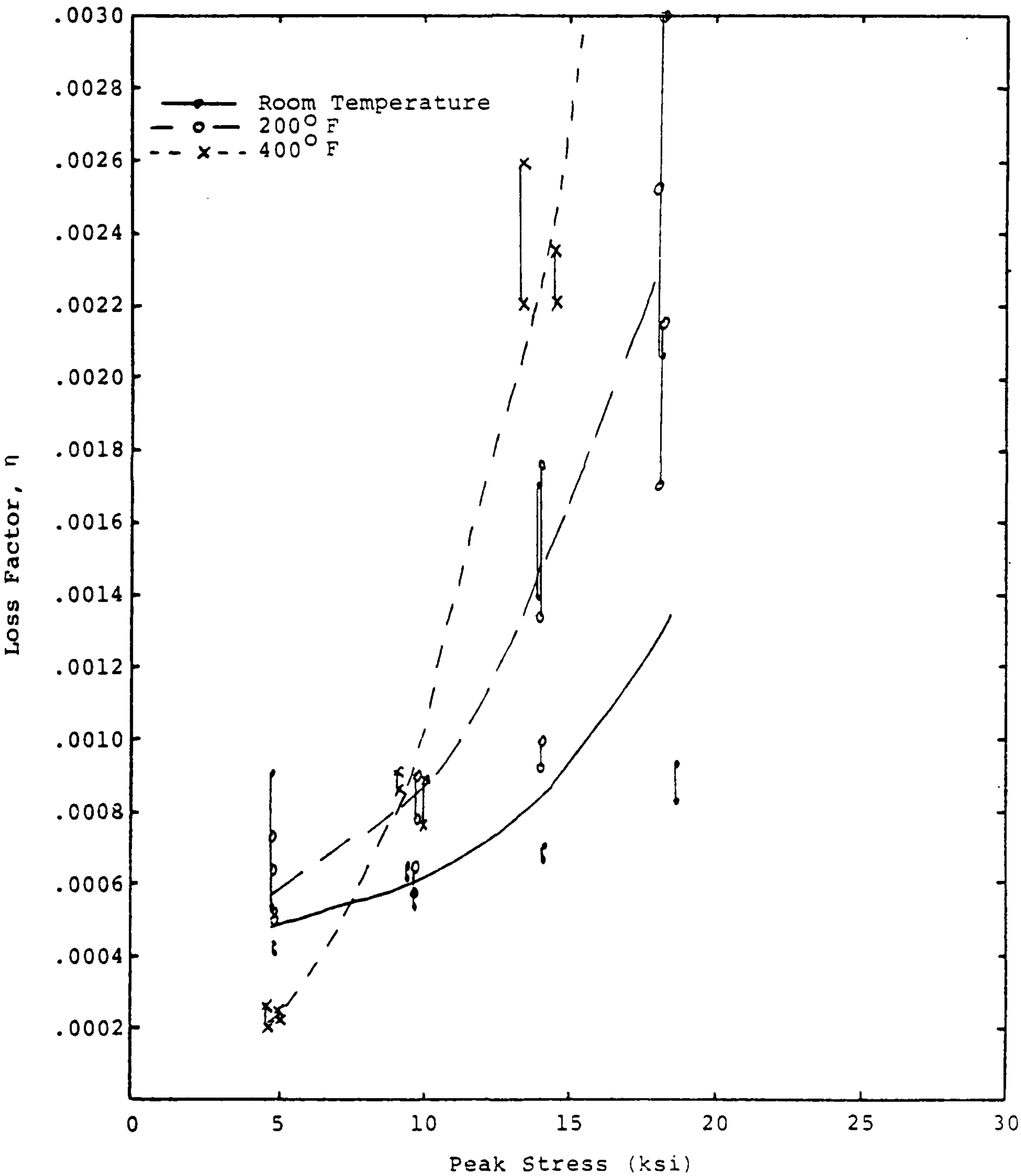

Figure 20

EFFECTS OF STRESS AND TEMPERATURE
$FP(Al_2O_3)$/ZE41A MAGNESIUM
56 v/o, 0° FIBER ORIENTATION, AS CAST

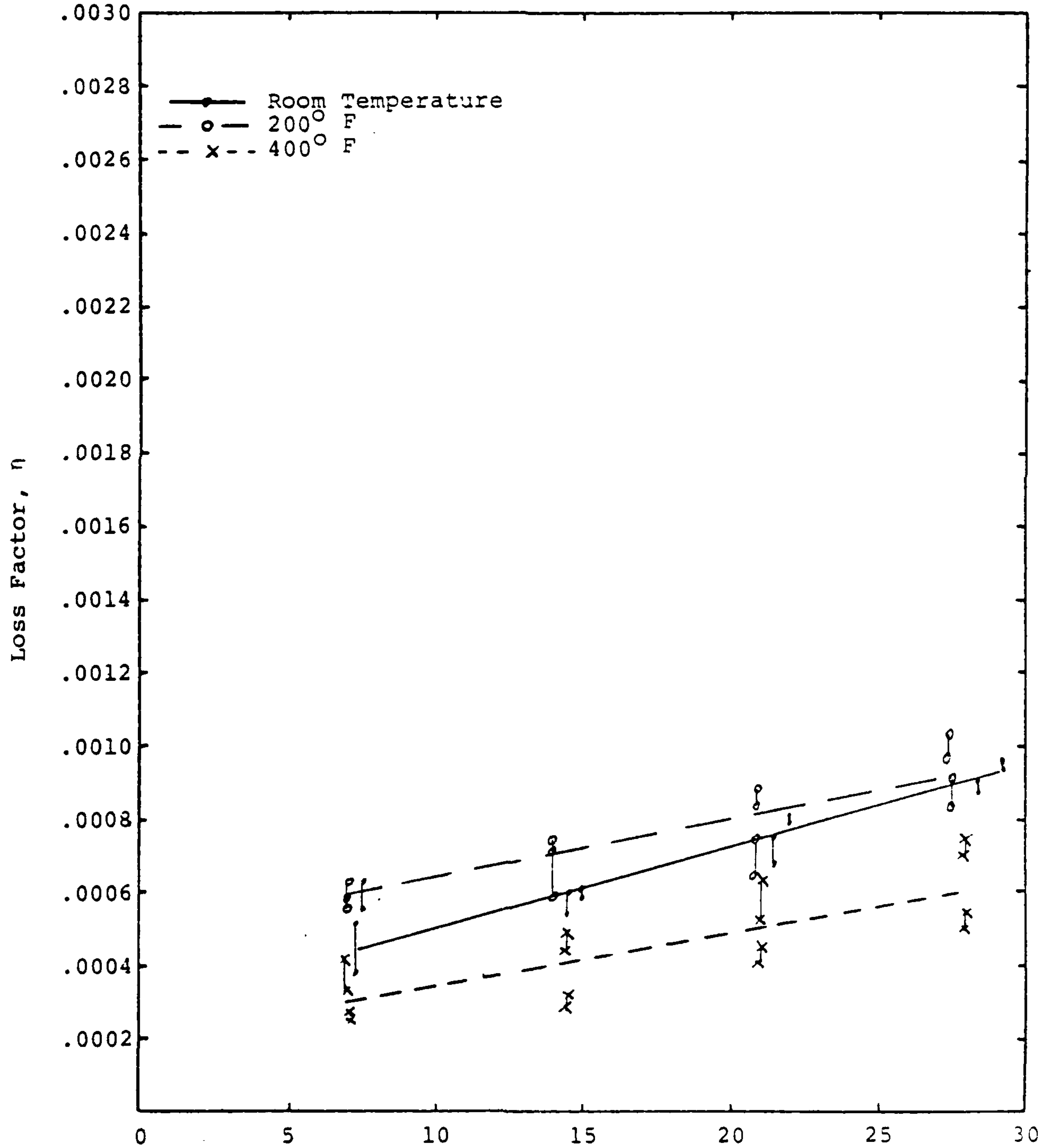

Figure 21

EFFECTS OF STRESS AND TEMPERATURE
$FP(Al_2O_3)$/ZE41A MAGNESIUM
56 v/o, 0^o FIBER ORIENTATION, T-5 HEAT TREATED

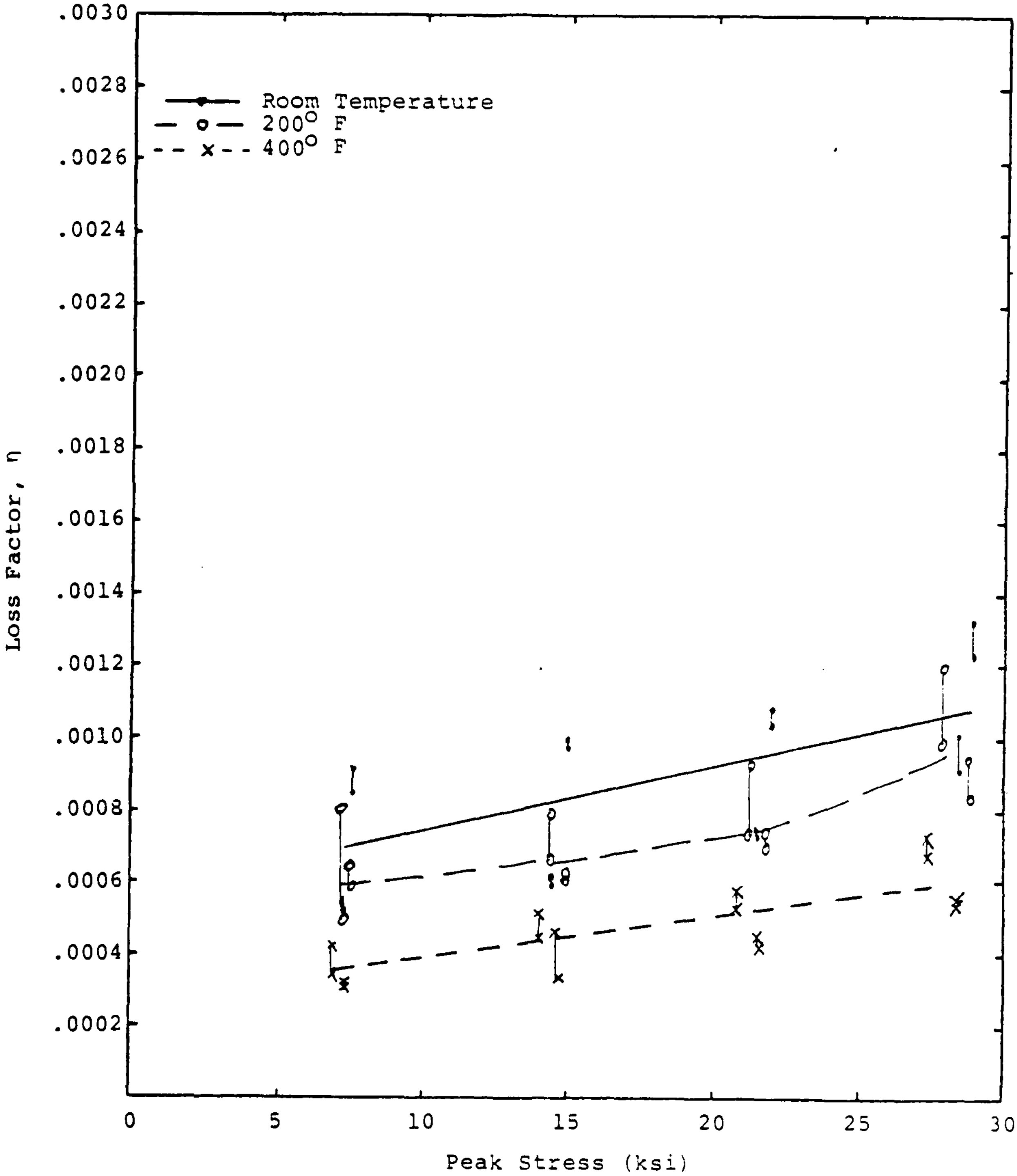

Figure 22

EFFECTS OF STRESS AND TEMPERATURE
FP(Al_2O_3)/ZE41A MAGNESIUM
56 v/o, ±22½° FIBER ORIENTATION, AS CAST

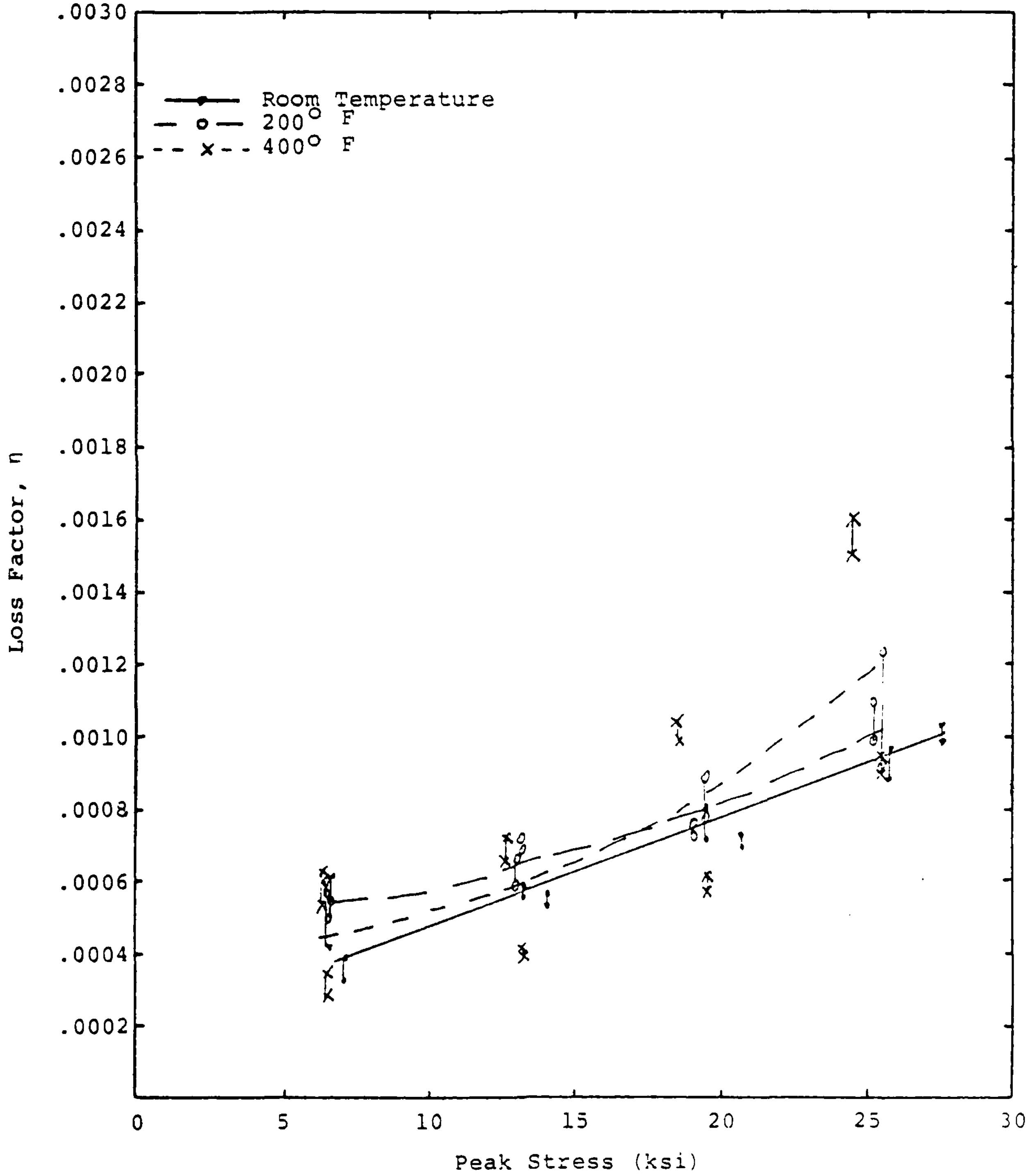

Figure 23

EFFECTS OF STRESS AND TEMPERATURE
FP(Al_2O_3)/ZE41A MAGNESIUM
56 v/o, ±22½° FIBER ORIENTATION, T-5 HEAT TREATED

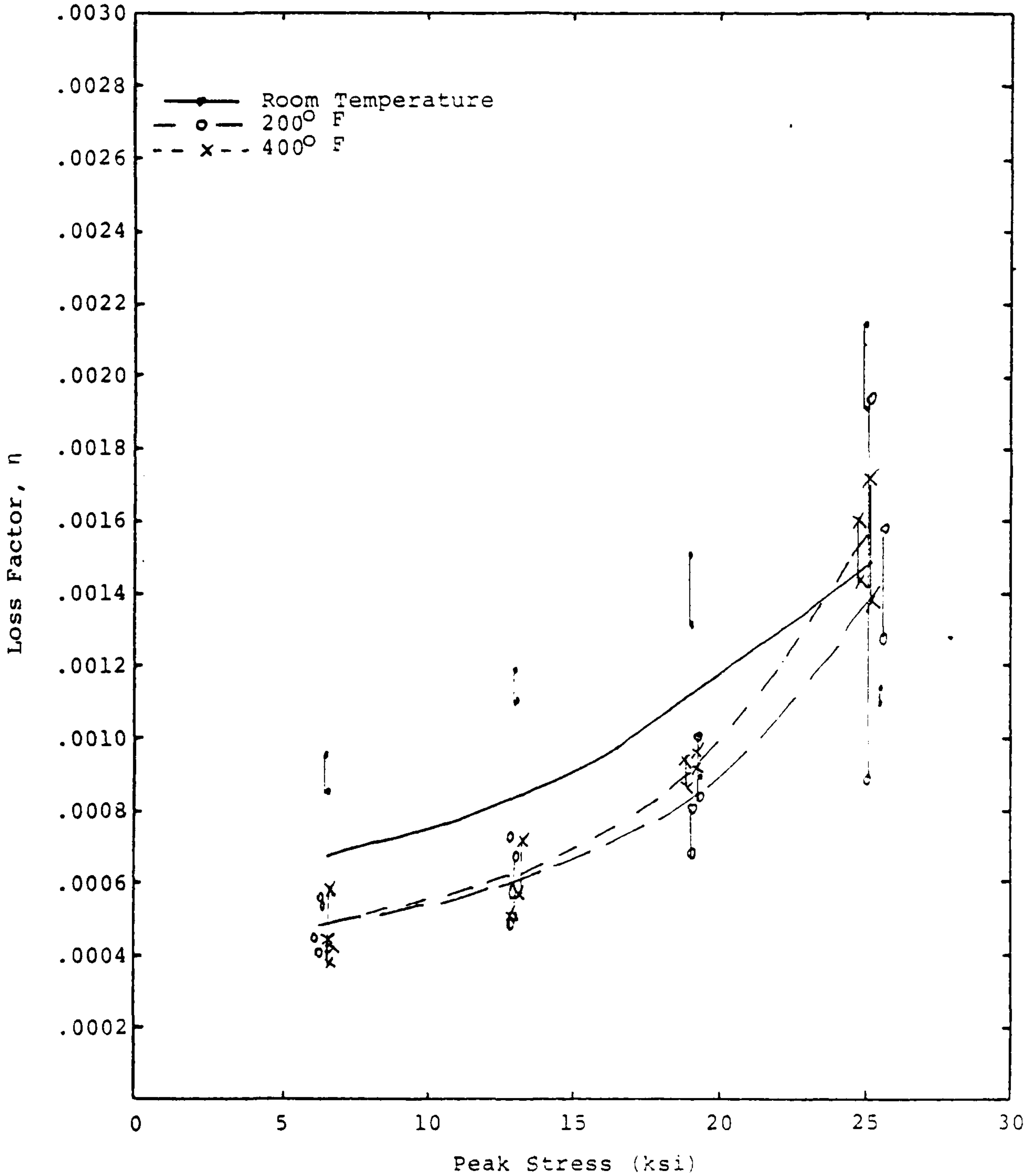

Figure 24

APPENDIX A
CERTIFICATION OF HEAT TREATMENT

QUALITY TOOL, DIE AND PRODUCTION HARDENING

ALUMINUM . . . BRONZE . . . MAGNESIUM . . . STEEL

industrial heat treating, inc.

22-26 DENSMORE STREET • P.O. BOX 98 • NORTH QUINCY, MASSACHUSETTS 02171
AREA CODE (617) 328-1010

MAY 17, 1983

BOLT BERANEK & NEWMAN INC.
50 MOULTON ST.
CAMBRIDGE, MA 02238

Gentlemen:

This is to certify that 30 pcs., ZE41A Magnesium Matrix Composite Samples,

was/were processed as shown below and shipped under our S.M. B020080

Aged for 2½ hrs., at 650°F., air cooled.
Per P.O. & MIL-M-6857.

The above material was on your order No. 34685

and applies to Government Contract DAAAG46-82-C-0060

Very truly yours,

INDUSTRIAL HEAT TREATING, INC.,

Paul J. Brooks

Notary Willard M. Davis

APPENDIX B

STANDARD BEAM EQUATIONS

APPENDIX B. STANDARD BEAM EQUATIONS

The material frequencies of a cantilever beam of length L (in.) and thickness h(in.) are [8]:

$$f_1 = \frac{1}{2\pi} \left(\frac{1.8751}{L}\right)^2 h \left(\frac{32E}{\rho}\right)^{\frac{1}{2}}$$

$$f_2 = 6.36 f_1$$

$$f_3 = 17.53 f_1$$

$$f_4 = 34.38 f_1$$

$$f_5 = 56.82 f_1$$

where

E = Young's modulus (psi) and

ρ = material density (lb_m/in^3).

The tip amplitude as a function of specimen stress and material properties is given by:

$$Y_{t,DA} = A_n \left(\frac{\sigma_o}{f_n}\right) \frac{1}{\sqrt{E\rho}}$$

where

$Y_{t,DA}$ = peak-to-peak amplitude (in)

σ_o = maximum stress (psi)

f_n = specimen natural frequency (Hz), and

A_1 = 3.63

A_2 = 3.747

A_3 = 1.808

A_4 = 1.306

A_5 = 2.224

APPENDIX C

TABULAR RESULTS OF PHASES 1 AND 2

PHASE 1 RESULTS: ROOM TEMPERATURE

Sample No.	Peak Sample Stress (ksi)	Natural Frequency (Hz)	Young's Modulus psi X 10^6	Avg. Sample Loss Factor	Max. Air Loss Factor ($X10^{-4}$)	Corrected Avg. Sample Loss Factor
1-1	6.1	147.7	23.8	3.12×10^{-3}	0.637	3.06×10^{-3}
	11.7	146.8	23.5	3.82×10^{-3}	1.25	3.70×10^{-3}
	20.3	145.3	23.2	4.99×10^{-3}	2.19	4.77×10^{-3}
	22.2	142.9	22.3	7.75×10^{-3}	2.49	7.5×10^{-3}
2-1	10.2	191.2	40.0	2.63×10^{-3}	0.637	2.57×10^{-3}
	18.7-18.8	185.5-185.9	37.7	5.62×10^{-3}	1.25	5.50×10^{-3}
	Sample Delaminated					
3-1	5.4	155.3	21.1	1.03×10^{-3}	0.803	$.95 \times 10^{-3}$
	10.4	154.4-154.7	20.9	1.56×10^{-3}	1.59	1.40×10^{-3}
	15.7	154.3-154.4	20.8	1.80×10^{-3}	2.36	1.56×10^{-3}
	20.6-20.7	153.7-154.0	20.7	2.38×10^{-3}	3.12	2.07×10^{-3}
4-1	9.0	200.7	35.2	1.58×10^{-3}	0.803	1.50×10^{-3}
	17.7-17.8	199.3-199.5	34.8	2.49×10^{-3}	1.59	2.33×10^{-3}
	23.4	198.2	34.3	3.04×10^{-3}	2.13	2.83×10^{-3}
5-1	7.9-8.0	146.4-146.8	31.9	3.73×10^{-4}	0.457	3.27×10^{-4}
	16.2	146.2-146.4	31.8	7.12×10^{-4}	0.94	6.18×10^{-4}
	23.8-23.9	145.9-146.0	31.7	1.25×10^{-3}	1.39	1.11×10^{-3}
	29.2	144.9-145.0	31.2	3.19×10^{-3}	1.73	3.02×10^{-3}
6-1	7.5	147.9-180.0	29.5	4.04×10^{-4}	0.518	3.52×10^{-4}
	15.0	147.9	29.5	5.53×10^{-4}	1.04	4.49×10^{-4}
	22.1-22.2	147.7-147.8	29.4	7.58×10^{-4}	1.53	6.05×10^{-4}
	28.2	147.6	29.3	1.00×10^{-3}	1.96	8.04×10^{-4}
7-1	7.7	149.4-149.5	30.1	4.30×10^{-4}	0.518	3.78×10^{-4}
	15.3	149.2-149.3	30.0	6.56×10^{-4}	1.04	5.52×10^{-4}
	22.2-22.5	149.0	29.9	9.81×10^{-4}	1.53	8.28×10^{-4}
	25.8	148.9	29.9	1.37×10^{-3}	1.76	1.19×10^{-3}
8-1	5.1	122.4-122.5	20.1	4.03×10^{-4}	0.521	3.51×10^{-4}
	10.2	122.4-122.5	20.1	5.04×10^{-4}	1.05	3.99×10^{-4}
	15.0-15.1	122.4	20.0	5.48×10^{-4}	1.54	3.94×10^{-4}
	19.9-20.0	122.3-122.4	20.0	8.28×10^{-4}	2.03	6.25×10^{-4}
9-1	7.8-8.0	109.4-109.5	15.7	4.78×10^{-4}	1.06	3.72×10^{-4}
	11.8	109.4-109.5	15.7	5.61×10^{-4}	1.57	4.04×10^{-4}
	15.6	109.4	15.7	6.95×10^{-4}	2.08	4.87×10^{-4}
	19.4	109.4	15.7	7.82×10^{-4}	2.59	5.23×10^{-4}
AL-1	4.2	144.2-144.3	10.3	4.78×10^{-4}	0.555	4.23×10^{-4}
	8.4	144.2	10.3	6.18×10^{-4}	1.11	5.07×10^{-4}
	12.4	144.2	10.3	7.69×10^{-4}	1.64	6.05×10^{-4}
	16.3-16.4	144.1-144.2	10.3	8.46×10^{-4}	2.17	6.29×10^{-4}
	20.3	144.1-144.2	10.3	1.12×10^{-3}	2.69	8.51×10^{-4}
	26.7	144.1	10.3	1.35×10^{-3}	3.53	9.97×10^{-4}
RZ-1	3.6-3.7	139.1-139.5	7.3	6.46×10^{-4}	2.90	3.56×10^{-4}
	5.5	139.1-139.2	7.2	8.09×10^{-4}	3.44	4.65×10^{-4}
	7.3	138.9-139.0	7.2	1.24×10^{-3}	5.32	7.08×10^{-4}
	9.0	138.8-139.0	7.2	1.67×10^{-3}	7.26	9.44×10^{-4}
CP-3	2.7-3.0	137.3-138.0	6.1	6.12×10^{-3}	1.07	6.01×10^{-3}
	4.5	136.2-136.6	5.9	6.00×10^{-3}	1.60	5.84×10^{-3}
	5.9	135.4-136.0	5.8	9.52×10^{-3}	2.14	9.31×10^{-3}
CP-1	6.7-6.8	133.4-133.9	5.7	1.16×10^{-2}	2.55	1.13×10^{-2}
	8.9-9.0	132.7	5.6	1.78×10^{-2}	3.36	1.75×10^{-2}
	Fatigue Failure					

PHASE 1 RESULTS: Nom. 200° F

Sample No.	Peak Sample Stress (ksi)	Natural Frequency (Hz)	Young's Modulus psi X 10^6	Avg. Sample Loss Factor	Max. Air Loss Factor ($X10^{-4}$)	Corrected Avg. Sample Loss Factor
1-2	6.0	146.5-146.7	23.5	5.77×10^{-4}	0.764	5.01×10^{-4}
	11.6	144.3-144.4	22.8	9.28×10^{-4}	1.53	7.75×10^{-4}
	16.6-16.7	141.9-142.3	22.1	1.36×10^{-3}	2.26	1.13×10^{-3}
	20.2-20.6	136.3-137.5	20.5	2.38×10^{-3}	2.98	2.08×10^{-3}
2-2	10.1	190.5-190.7	39.7	4.98×10^{-4}	0.764	4.22×10^{-4}
	19.7-19.8	187.9-188.4	38.7	1.06×10^{-3}	1.53	9.07×10^{-4}
	25.9-27.4 Delaminated	182.6-184.0	36.7	2.11×10^{-3}	2.26	1.88×10^{-3}
3-2	6.1	165.3	23.9	2.64×10^{-4}	0.954	1.69×10^{-4}
	11.8-12.1	164.9-165.0	23.8	3.25×10^{-4}	1.91	1.34×10^{-4}
	17.9	164.7-164.8	23.7	3.76×10^{-4}	2.82	0.94×10^{-4}
	23.4-23.5	164.0-164.3	23.6	5.48×10^{-4}	3.72	1.76×10^{-4}
4-2	8.5	195.2-195.3	33.3	5.07×10^{-4}	0.954	4.12×10^{-4}
	16.6-16.9	194.2-194.4	33.0	8.35×10^{-4}	1.91	6.44×10^{-4}
	22.6-22.9	193.0-193.4	32.7	1.08×10^{-3}	2.60	8.20×10^{-4}
5-2	8.0	145.5-145.6	31.5	2.23×10^{-4}	0.561	1.67×10^{-4}
	16.0	145.3-145.4	31.4	3.64×10^{-4}	1.12	2.52×10^{-4}
	23.6	145.1	31.3	7.21×10^{-4}	1.66	5.55×10^{-4}
	27.9-29.1	144.4-144.6	31.1	9.78×10^{-4}	2.01	7.77×10^{-4}
6-2	7.6	148.5-148.7	29.8	2.50×10^{-4}	0.62	1.88×10^{-4}
	15.2	148.5-148.6	29.7	1.86×10^{-4}	1.24	0.62×10^{-4}
	22.0-22.3	148.5	29.7	2.03×10^{-4}	1.82	0.21×10^{-4}
	28.1-28.4	148.3-148.4	29.7	2.25×10^{-4}	2.10	0.15×10^{-4}
7-2	7.7	149.3	30.0	1.40×10^{-4}	0.62	7.8×10^{-5}
	15.3	149.2-149.3	30.0	1.94×10^{-4}	1.24	7.0×10^{-5}
	22.5-22.6	149.0-149.1	29.9	2.76×10^{-4}	1.83	9.3×10^{-5}
	26.5-26.9	148.8-148.9	29.9	3.27×10^{-4}	2.16	1.11×10^{-4}
8-2	7.2	145.1	28.1	2.59×10^{-4}	0.625	1.97×10^{-4}
	14.3-14.4	145.0-145.1	28.1	3.33×10^{-4}	1.25	2.08×10^{-4}
	21.1-21.2	144.9-145.0	28.1	4.19×10^{-4}	1.84	2.35×10^{-4}
	26.5-26.6	144.6-144.8	28.0	4.18×10^{-4}	2.32	1.86×10^{-4}
9-2	3.9-4.0	108.6-108.7	15.5	4.65×10^{-4}	0.636	4.01×10^{-4}
	7.9	108.6-108.7	15.5	4.77×10^{-4}	1.27	3.50×10^{-4}
	11.6	108.5-108.6	15.5	5.29×10^{-4}	1.88	3.41×10^{-4}
	15.4	108.5	15.4	5.44×10^{-4}	2.48	2.96×10^{-4}
	19.1	108.4	15.4	6.65×10^{-4}	3.09	3.56×10^{-4}
AL-2	5.0	142.0-142.2	10.0	3.58×10^{-4}	0.82	2.76×10^{-4}
	7.6-7.7	142.1	10.0	3.74×10^{-4}	1.23	2.51×10^{-4}
	10.1-10.3	142.0-142.1	10.0	4.01×10^{-4}	1.64	2.37×10^{-4}
	12.4-12.6	141.9-142.0	10.0	4.24×10^{-4}	2.02	2.22×10^{-4}
RZ-2	3.6	138.3-138.8	7.2	6.81×10^{-4}	1.09	5.72×10^{-4}
	5.4	138.6-138.7	7.2	8.85×10^{-4}	1.63	7.22×10^{-4}
	7.2	138.2-138.5	7.2	2.25×10^{-3}	2.17	2.03×10^{-3}
	8.8	137.6-138.1	7.1	3.28×10^{-3}	2.67	3.01×10^{-3}
CP-2	2.8	132.2-132.5	5.6	5.28×10^{-3}	1.28	5.15×10^{-3}
	4.1	130.4-131.3	5.5	9.62×10^{-3}	1.91	9.43×10^{-3}
	5.4	129.6-130.3	5.4	1.38×10^{-2}	2.55	1.32×10^{-2}
	5.9-6.3 Failure	122.6-126.4	5.0	1.73×10^{-2}	3.14	1.76×10^{-2}

PHASE 1 RESULTS: 400° F

Sample No.	Peak Sample Stress (ksi)	Natural Frequency (Hz)	Young's Modulus psi X 10^6	Avg. Sample Loss Factor	Max. Air Loss Factor (X10^{-4})	Corrected Avg. Sample Loss Factor
1-3	6.4	151.5-151.9	25.2	5.11×10^{-4}	0.345	4.77×10^{-4}
	12.2-12.3	150.0-150.3	24.7	9.15×10^{-4}	0.692	8.46×10^{-4}
	17.9-18.0	147.5-148.0	23.9	1.61×10^{-3}	1.02	1.51×10^{-3}
	22.9-23.5	144.9-146.8	23.2	2.46×10^{-3}	1.35	2.33×10^{-3}
2-3	10.6	194.7-194.8	41.5	6.01×10^{-4}	0.345	5.67×10^{-4}
	19.4-19.7	186.7-188.0	38.4	2.02×10^{-3}	0.692	1.95×10^{-3}
	24.0-25.0	170.9-174.4	32.5	4.54×10^{-3}	1.02	4.44×10^{-3}
3-3	6.0	164.0-164.1	23.5	3.29×10^{-4}	0.433	2.86×10^{-4}
	12.0	163.7-163.8	23.4	3.79×10^{-4}	0.867	2.92×10^{-4}
	17.5-17.6	163.2-163.3	23.3	5.04×10^{-4}	1.28	3.76×10^{-4}
	22.7-22.8	161.6-161.9	22.9	5.66×10^{-4}	1.68	3.98×10^{-4}
4-3	8.9	199.5-199.6	34.8	5.97×10^{-4}	0.433	5.54×10^{-4}
	17.6	198.6	34.5	5.13×10^{-4}	0.867	4.26×10^{-4}
	22.4-22.8	196.0-197.6	33.8	1.09×10^{-3}	1.136	9.77×10^{-4}
5-3	7.8	143.1-143.2	30.5	2.05×10^{-4}	0.254	1.80×10^{-4}
	15.5	142.8-142.9	30.3	2.60×10^{-4}	0.508	2.09×10^{-4}
	22.7-22.8	142.4-142.7	30.2	5.30×10^{-4}	0.752	4.55×10^{-4}
	28.9-29.6	141.4-141.5	29.7	9.54×10^{-4}	0.972	8.57×10^{-4}
6-3	7.6	148.3-148.4	29.7	2.71×10^{-4}	0.281	2.43×10^{-4}
	15.1	148.0-148.2	29.6	3.87×10^{-4}	0.560	3.31×10^{-4}
	22.1-22.2	147.7-147.8	29.4	4.52×10^{-4}	0.829	3.69×10^{-4}
	28.0-28.1	147.2-147.3	29.2	5.28×10^{-4}	1.06	4.22×10^{-4}
7-3	7.5	148.0-148.1	29.5	2.53×10^{-4}	0.281	2.25×10^{-4}
	15.0	147.7-147.8	29.4	3.88×10^{-4}	0.560	3.32×10^{-4}
	22.0	147.1-147.4	29.2	6.88×10^{-4}	0.829	6.05×10^{-4}
	28.0-28.1	146.2-146.5	28.9	9.24×10^{-4}	1.08	8.15×10^{-4}
8-3	5.7	129.6-129.7	22.5	5.24×10^{-4}	0.282	4.96×10^{-4}
	11.4-11.5	129.5-129.6	22.4	6.00×10^{-4}	0.565	5.44×10^{-4}
	16.8	129.2	22.3	6.11×10^{-4}	0.834	5.28×10^{-4}
	22.1-22.2	128.9-129.0	22.2	7.80×10^{-4}	1.10	6.70×10^{-4}
9-3	7.2	103.5-103.9	14.1	7.33×10^{-4}	0.576	6.75×10^{-4}
	10.6	103.6-103.8	14.1	6.74×10^{-4}	0.851	5.89×10^{-4}
	14.0	103.7	14.1	6.72×10^{-4}	1.13	5.59×10^{-4}
	17.1	103.8	14.1	6.39×10^{-4}	1.37	5.02×10^{-4}
AL-3	4.1	128.4-128.6	8.2	4.24×10^{-4}	0.369	3.87×10^{-4}
	6.2	128.4	8.2	4.17×10^{-4}	0.554	3.62×10^{-4}
	8.2	128.2-128.3	8.1	4.63×10^{-4}	0.741	3.89×10^{-4}
	10.1	128.3	8.1	4.67×10^{-4}	0.911	3.76×10^{-4}
RZ-3	3.3	131.5	6.5	5.97×10^{-4}	0.492	5.48×10^{-4}
	4.8	130.8-131.0	6.4	1.52×10^{-3}	0.736	1.45×10^{-3}
	6.4	130.0-130.5	6.3	3.42×10^{-3}	0.983	3.32×10^{-3}
	7.7	128.8-129.2	6.2	5.75×10^{-3}	1.21	5.63×10^{-3}
CP-3	2.7	129.6-130.2	5.4	9.53×10^{-3}	0.576	9.47×10^{-3}
	3.8	125.2-125.7	5.0	1.31×10^{-2}	0.867	1.30×10^{-2}
	4.9	123.3	4.9	2.22	1.16	2.22
	Fatigue Failure					

PHASE 2 RESULTS: As Cast Samples at Room Temperature

Sample No.	Peak Sample Stress (ksi)	Natural Frequency (Hz)	Young's Modulus psi X 10^6	Avg. Sample Loss Factor	Max. Air Loss Factor ($X10^{-4}$)	Corrected Avg. Sample Loss Factor
A-1	6.3	146.4-146.6	24.8	8.08×10^{-4}	2.14	5.94×10^{-4}
	12.6-12.7	146.4-146.5	24.8	7.46×10^{-4}	4.27	3.19×10^{-4}
	18.4-18.6	146.3	24.8	7.55×10^{-4}	6.31	1.24×10^{-4}
	24.0-24.6	146.0-146.2	24.7	1.08×10^{-3}	8.35	2.49×10^{-4}
A-7	5.8	140.9-141.0	22.6	4.74×10^{-4}	2.17	2.57×10^{-4}
	11.5	140.8	22.6	7.63×10^{-4}	4.33	3.30×10^{-4}
	17.0	140.7	22.6	8.45×10^{-4}	6.40	2.05×10^{-4}
	22.4-22.5	140.4-140.6	22.5	1.09×10^{-3}	8.46	2.44×10^{-4}
B-1	4.7	125.4-125.5	18.4	5.98×10^{-4}	2.12	3.86×10^{-4}
	9.4	125.3-125.4	18.4	6.98×10^{-4}	4.23	2.75×10^{-4}
	13.8	125.1-125.2	18.3	1.03×10^{-3}	6.25	4.01×10^{-4}
	18.1-18.2	124.9-125.0	18.2	1.56×10^{-3}	8.26	7.34×10^{-4}
C-1	5.0	128.8	19.5	4.17×10^{-4}	2.10	2.07×10^{-4}
	9.9-10.0	128.6-128.8	19.5	6.02×10^{-4}	4.20	1.82×10^{-4}
	14.6-14.7	128.5-128.6	19.5	6.33×10^{-4}	6.20	1.3×10^{-5}
	19.4	128.5-128.6	19.4	8.95×10^{-4}	8.20	7.5×10^{-5}
D-1	7.3	147.0	28.6	4.20×10^{-4}	1.87	2.33×10^{-4}
	14.6-14.7	147.2-147.3	28.7	5.47×10^{-4}	3.73	1.74×10^{-4}
	21.6	147.2	28.7	7.11×10^{-4}	5.51	1.60×10^{-4}
	28.5-28.6	147.1-147.2	28.7	8.77×10^{-4}	7.29	1.48×10^{-4}
D-7	7.5	148.6	29.4	5.73×10^{-4}	1.86	3.87×10^{-4}
	15.0	148.5	29.4	5.99×10^{-4}	3.71	2.28×10^{-4}
	22.1	148.4	29.3	7.99×10^{-4}	5.48	2.51×10^{-4}
	29.3	148.4-148.5	29.4	9.47×10^{-4}	7.25	2.22×10^{-4}
E/J-3	6.6	139.5-139.7	26.0	5.46×10^{-4}	1.85	3.61×10^{-4}
	13.2	139.3-139.4	25.9	5.80×10^{-4}	3.71	2.09×10^{-4}
	19.5	139.2-139.3	25.9	7.83×10^{-4}	5.48	2.35×10^{-4}
	25.7	139.2	25.8	9.45×10^{-4}	7.24	2.21×10^{-4}
F-1	7.1	143.1-143.2	27.7	3.77×10^{-4}	1.83	1.94×10^{-4}
	14.1	143.0	27.6	5.60×10^{-4}	3.66	1.94×10^{-4}
	20.8	142.9-143.0	27.6	7.24×10^{-4}	5.41	1.83×10^{-4}
	27.5	142.9	27.6	1.03×10^{-3}	7.15	3.15×10^{-4}

PHASE 2 RESULTS: Heat Treated (T-5) Samples at Room Temperature

Sample No.	Peak Sample Stress (ksi)	Natural Frequency (Hz)	Young's Modulus psi X 10^6	Avg. Sample Loss Factor	Max. Air Loss Factor ($X10^{-4}$)	Corrected Avg. Sample Loss Factor
A-2	5.5	137.7	21.5	4.10×10^{-4}	2.18	1.92×10^{-4}
	10.9	137.6	21.4	5.00×10^{-4}	4.37	0.63×10^{-4}
	16.1	137.4-137.5	21.4	7.26×10^{-4}	6.44	0.82×10^{-4}
	21.3	137.4-137.5	21.4	8.38×10^{-4}	8.01	0.37×10^{-4}
A-8	6.0	142.9	23.5	3.96×10^{-4}	2.15	1.81×10^{-4}
	12.0	142.8-142.9	23.5	7.60×10^{-4}	4.30	3.30×10^{-4}
	17.6	142.7	23.4	1.03×10^{-3}	6.35	3.95×10^{-4}
	23.2-23.3	142.5-142.6	23.4	1.22×10^{-3}	8.40	3.80×10^{-4}
B-4	4.7	124.9-125.0	18.4	6.86×10^{-4}	2.10	4.76×10^{-4}
	9.4	124.9-125.1	18.4	6.20×10^{-4}	4.20	2.00×10^{-4}
	13.7-13.8	124.5-124.7	18.3	1.57×10^{-3}	6.21	9.49×10^{-4}
	18.0-18.1	123.9-124.4	18.2	2.70×10^{-3}	8.21	1.88×10^{-3}
C-2	4.8	126.8	18.8	3.96×10^{-4}	2.09	1.87×10^{-4}
	9.6	126.7	18.7	5.39×10^{-4}	4.18	1.21×10^{-4}
	14.1	126.6	18.7	6.70×10^{-4}	6.18	0.52×10^{-4}
	18.6	126.5-126.6	18.6	8.67×10^{-4}	8.17	0.50×10^{-4}
D-2	7.3	146.9	28.8	5.73×10^{-4}	1.86	3.87×10^{-4}
	14.6	146.6-146.7	28.8	5.99×10^{-4}	3.72	2.27×10^{-4}
	21.5	146.6-146.7	28.7	7.30×10^{-4}	5.49	1.81×10^{-4}
	28.4-28.5	146.5-146.6	28.7	9.47×10^{-4}	7.26	2.21×10^{-4}
D-8	7.5	148.9-149.1	29.5	8.78×10^{-4}	1.86	6.92×10^{-4}
	15.0	148.8-148.9	29.4	9.81×10^{-4}	3.72	6.09×10^{-4}
	22.1	148.5-148.6	29.3	1.07×10^{-3}	5.50	5.20×10^{-4}
	29.2	148.5	29.3	1.27×10^{-3}	7.27	5.43×10^{-4}
E/J-4	6.55	139.2-139.3	25.8	4.25×10^{-4}	1.87	2.38×10^{-4}
	13.1	139.1	25.8	7.01×10^{-4}	3.73	3.28×10^{-4}
	19.3	139.0-139.1	25.7	8.83×10^{-4}	5.51	3.32×10^{-4}
	25.5	139.0	25.7	1.14×10^{-3}	7.29	4.11×10^{-4}
F-2	6.5	137.5-137.6	25.6	9.00×10^{-4}	1.84	7.16×10^{-4}
	13.0	137.5-137.6	25.6	1.15×10^{-3}	3.68	7.82×10^{-4}
	19.1	137.4-137.5	25.5	1.39×10^{-3}	5.43	8.47×10^{-4}
	25.0-25.1	136.7-137.0	25.3	2.05×10^{-3}	7.18	1.33×10^{-3}

PHASE 2 RESULTS: As Cast Samples at 200° F

Sample No.	Peak Sample Stress (ksi)	Natural Frequency (Hz)	Young's Modulus psi X 10^6	Avg. Sample Loss Factor	Max. Air Loss Factor ($X10^{-4}$)	Corrected Avg. Sample Loss Factor
A-3	5.6	138.8-138.9	22.0	6.99×10^{-4}	1.46	5.53×10^{-4}
	11.2	138.6-138.8	22.0	7.77×10^{-4}	2.92	4.85×10^{-4}
	16.5	138.6	21.9	8.89×10^{-4}	4.31	4.58×10^{-4}
	21.8	138.4-138.5	21.9	9.12×10^{-4}	5.70	3.42×10^{-4}
A-9	5.8	140.6-140.7	22.9	5.57×10^{-4}	1.44	4.13×10^{-4}
	11.6-11.7	140.5-140.6	22.8	8.22×10^{-4}	2.89	5.33×10^{-4}
	17.2	140.4-140.5	22.8	1.00×10^{-3}	4.26	5.76×10^{-4}
	22.7	140.4-140.5	22.8	1.20×10^{-3}	5.64	6.36×10^{-4}
B-3	4.7	124.8-124.9	18.4	7.72×10^{-4}	1.42	6.30×10^{-4}
	9.3	124.6-124.7	18.3	8.75×10^{-4}	2.83	5.92×10^{-4}
	13.8	124.6-124.7	18.3	1.21×10^{-3}	4.18	7.92×10^{-4}
	18.2	124.5-124.6	18.3	2.37×10^{-3}	5.53	1.82×10^{-3}
B-7	4.6	124.3-124.4	18.1	8.10×10^{-4}	1.43	6.67×10^{-4}
	9.2	124.1-124.3	18.0	9.39×10^{-4}	2.86	6.53×10^{-4}
	13.5	123.9-124.1	18.0	1.26×10^{-3}	4.22	8.38×10^{-4}
	17.8	123.8-123.9	17.9	1.96×10^{-3}	5.58	1.40×10^{-3}
D-3	7.1	144.5	27.8	6.01×10^{-4}	1.25	4.76×10^{-4}
	14.1-14.2	144.3-144.4	27.7	7.29×10^{-4}	2.51	4.78×10^{-4}
	20.8-20.9	144.2-144.3	27.7	8.63×10^{-4}	3.70	4.93×10^{-4}
	27.6	144.3	27.7	9.75×10^{-4}	4.89	4.86×10^{-4}
D-9	7.1	144.6-144.7	27.8	5.61×10^{-4}	1.26	4.35×10^{-4}
	14.1-14.2	144.4-144.5	27.8	6.53×10^{-4}	2.51	4.02×10^{-4}
	20.9	144.4	27.7	6.90×10^{-4}	3.71	3.19×10^{-4}
	27.6	144.3	27.7	8.61×10^{-4}	4.90	3.71×10^{-4}
E/J-5	6.5	138.3	25.6	5.98×10^{-4}	1.25	4.73×10^{-4}
	13.0	138.0-138.1	25.5	6.37×10^{-4}	2.50	3.87×10^{-4}
	19.1	137.8-137.9	25.4	7.52×10^{-4}	3.69	3.83×10^{-4}
	25.2-25.3	137.7-137.8	25.3	1.04×10^{-3}	4.88	5.50×10^{-4}
F-3	6.6	139.1-139.2	25.9	5.39×10^{-4}	1.25	4.14×10^{-4}
	13.1-13.2	138.9-139.0	25.8	7.13×10^{-4}	2.50	4.63×10^{-4}
	19.4	138.8-138.9	25.8	8.66×10^{-4}	3.69	4.97×10^{-4}
	25.6-25.7	138.8-138.9	25.7	1.15×10^{-3}	4.88	6.62×10^{-4}

PHASE 2 RESULTS: Heat Treated (T-5) Samples at 200° F

Sample No.	Peak Sample Stress (ksi)	Natural Frequency (Hz)	Young's Modulus psi X 10^6	Avg. Sample Loss Factor	Max. Air Loss Factor ($X10^{-4}$)	Corrected Avg. Sample Loss Factor
A-4	5.7	139.2-139.3	22.3	5.21×10^{-4}	1.45	3.76×10^{-4}
	11.3-11.4	139.1-139.2	22.3	6.78×10^{-4}	2.90	3.88×10^{-4}
	16.7	138.9	22.2	8.25×10^{-4}	4.29	3.96×10^{-4}
	22.1	138.9-139.0	22.2	8.70×10^{-4}	5.67	3.03×10^{-4}
A-10	5.8	140.0-140.2	22.7	6.77×10^{-4}	1.44	5.33×10^{-4}
	11.5	139.8-139.9	22.6	7.54×10^{-4}	2.39	4.65×10^{-4}
	17.0	139.7-139.9	22.6	9.61×10^{-4}	4.26	5.35×10^{-4}
	22.4-22.5	139.6-139.7	22.5	1.05×10^{-3}	5.64	4.83×10^{-4}
B-2	4.7	125.1-125.2	18.5	5.62×10^{-4}	1.41	4.21×10^{-4}
	9.4	125.1	18.5	7.32×10^{-4}	2.83	4.49×10^{-4}
	13.9	124.9-125.0	18.4	1.29×10^{-3}	4.17	8.73×10^{-4}
	18.2	124.4-124.5	18.3	2.62×10^{-3}	5.52	2.07×10^{-3}
B-8	4.7	126.0-126.1	18.4	6.09×10^{-4}	1.44	4.65×10^{-4}
	9.4	125.9-126.0	18.4	7.32×10^{-4}	2.88	4.44×10^{-4}
	13.8	125.6-125.8	18.3	1.16×10^{-3}	4.25	7.35×10^{-4}
	18.1-18.2	125.2-125.5	18.2	2.00×10^{-3}	5.62	1.44×10^{-3}
D-4	7.5	148.5-148.6	29.4	6.11×10^{-4}	1.25	4.86×10^{-4}
	15.0	148.4	29.4	6.17×10^{-4}	2.49	3.68×10^{-4}
	22.1	148.2-148.3	29.3	7.20×10^{-4}	3.68	3.52×10^{-4}
	29.1-29.2	148.1-148.2	29.3	8.81×10^{-4}	4.87	3.94×10^{-4}
D-10	7.3	146.2-146.3	28.5	6.38×10^{-4}	1.25	5.13×10^{-4}
	14.5	146.0	28.4	7.36×10^{-4}	2.51	4.85×10^{-4}
	21.3-21.4	145.9-146.0	28.4	8.32×10^{-4}	3.70	4.62×10^{-4}
	28.2	145.8-145.9	28.3	1.06×10^{-3}	4.90	5.70×10^{-4}
E/J-6	6.6	138.6	25.7	5.38×10^{-4}	1.25	4.13×10^{-4}
	13.1	138.4-138.5	25.6	6.97×10^{-4}	2.50	4.47×10^{-4}
	19.3	138.3-138.4	25.6	9.29×10^{-4}	3.68	5.61×10^{-4}
	25.4-25.5	138.1-138.3	25.5	1.42×10^{-3}	4.87	9.33×10^{-4}
F-4	6.4	137.3	25.3	4.38×10^{-4}	1.25	3.13×10^{-4}
	12.9	137.2	25.2	5.42×10^{-4}	2.49	2.93×10^{-4}
	19.0	137.1	25.2	7.44×10^{-4}	3.68	3.76×10^{-4}
	25.0	137.0	25.1	1.31×10^{-3}	4.87	8.24×10^{-4}

PHASE 2 RESULTS: As Cast Samples at 400° F

Sample No.	Peak Sample Stress (ksi)	Natural Frequency (Hz)	Young's Modulus psi X 10^6	Avg. Sample Loss Factor	Max. Air Loss Factor (X10^{-4})	Corrected Avg. Sample Loss Factor
A-5	5.6	139.1-139.3	22.1	2.87×10^{-4}	1.21	1.66×10^{-4}
	11.2	138.9-139.0	22.0	3.36×10^{-4}	2.42	0.94×10^{-4}
	16.6	138.9	22.0	4.24×10^{-4}	3.58	0.66×10^{-4}
	21.8-21.9	138.6-138.8	21.9	4.93×10^{-4}	4.73	0.20×10^{-4}
A-11	5.9	141.5	23.1	3.94×10^{-4}	1.19	2.75×10^{-4}
	11.8	141.5-141.7	23.1	5.31×10^{-4}	2.39	2.92×10^{-4}
	17.4	141.3-141.5	23.1	6.22×10^{-4}	3.53	2.69×10^{-4}
	23.0	141.2-141.3	23.0	7.52×10^{-4}	4.66	2.86×10^{-4}
B-5	4.6	123.2-123.4	17.9	2.25×10^{-4}	1.17	1.08×10^{-4}
	9.1	123.1-123.3	17.8	3.91×10^{-4}	2.35	1.56×10^{-4}
	13.3	122.6-122.7	17.7	9.55×10^{-4}	3.47	6.08×10^{-4}
	17.2-17.6	121.5-122.1	17.5	1.94×10^{-3}	4.58	1.48×10^{-3}
B-9	4.7	126.1-126.3	18.6	3.06×10^{-4}	1.18	1.88×10^{-4}
	9.4-9.5	125.9-126.1	18.5	5.41×10^{-4}	2.37	3.04×10^{-4}
	13.8	125.3-125.5	18.4	1.55×10^{-3}	3.50	1.20×10^{-3}
	18.0-18.1	124.5-124.8	18.1	2.72×10^{-3}	4.62	2.26×10^{-3}
D-5	7.2	146.6-146.7	28.4	2.57×10^{-4}	1.05	1.52×10^{-4}
	14.4-14.5	146.3-146.5	28.3	2.99×10^{-4}	2.09	0.90×10^{-4}
	21.3	146.2-146.4	28.3	4.23×10^{-4}	3.09	1.14×10^{-4}
	28.1	146.1-146.2	28.2	5.12×10^{-4}	4.08	1.04×10^{-4}
D-11	7.2	144.7-144.9	28.2	3.63×10^{-4}	1.03	2.60×10^{-4}
	14.3-14.4	144.6-144.8	28.1	4.50×10^{-4}	2.06	2.44×10^{-4}
	21.1-21.2	144.6-144.7	28.1	5.73×10^{-4}	3.04	2.69×10^{-4}
	27.9	144.4-144.5	28.0	7.17×10^{-4}	4.02	3.15×10^{-4}
E/J-1	6.6	138.8-139.0	26.0	3.35×10^{-4}	1.03	2.32×10^{-4}
	13.2	138.7	25.9	4.23×10^{-4}	2.05	2.18×10^{-4}
	19.4-19.5	138.4-138.6	25.8	6.11×10^{-4}	3.03	3.08×10^{-4}
	25.6	138.2-138.3	25.7	9.45×10^{-4}	4.00	5.45×10^{-4}
E/J-7	6.3	136.3-136.5	24.9	6.14×10^{-4}	1.03	5.11×10^{-4}
	12.6-12.7	136.2-136.3	24.8	7.21×10^{-4}	2.07	5.14×10^{-4}
	18.6	135.9-136.1	24.7	1.04×10^{-3}	3.05	7.35×10^{-4}
	24.4-24.5	135.5-135.7	24.6	1.59×10^{-3}	4.04	1.19×10^{-3}

PHASE 2 RESULTS: Heat Treated (T-5) Samples at 400° F

Sample No.	Peak Sample Stress (ksi)	Natural Frequency (Hz)	Young's Modulus psi X 10^6	Sample Loss Factor	Max. Air Loss Factor (X10^{-4})	Min. Sample Loss Factor
A-6	5.5	136.2	21.4	3.92 X 10^{-4}	1.20	2.72 X 10^{-4}
	10.8-10.9	135.8-135.9	21.3	4.93 X 10^{-4}	2.40	2.53 X 10^{-4}
	15.9-16.0	135.5-135.7	21.2	6.13 X 10^{-4}	3.54	2.59 X 10^{-4}
	21.0	135.2-135.4	21.1	8.41 X 10^{-4}	4.68	3.73 X 10^{-4}
A-12	5.7-5.8	139.8-140.0	22.5	4.93 X 10^{-4}	1.20	3.73 X 10^{-4}
	11.4-11.5	139.7-139.8	22.5	5.39 X 10^{-4}	2.40	2.99 X 10^{-4}
	16.9	139.6-139.7	22.4	6.53 X 10^{-4}	3.54	2.99 X 10^{-4}
	22.3	139.4-139.6	22.4	8.38 X 10^{-4}	4.68	3.70 X 10^{-4}
B-6	4.9	128.1-128.2	19.2	2.24 X 10^{-4}	1.18	1.06 X 10^{-4}
	9.7-9.8	127.8-127.9	19.1	7.92 X 10^{-4}	2.36	5.56 X 10^{-4}
	14.2	126.9-127.0	18.9	2.24 X 10^{-3}	3.48	1.89 X 10^{-3}
	18.4-18.5	125.6-126.1	18.6	3.35 X 10^{-3}	4.61	2.89 X 10^{-3}
B-10	4.6	123.4-123.5	17.9	2.18 X 10^{-4}	1.18	1.00 X 10^{-4}
	9.1	123.1-123.2	17.8	8.76 X 10^{-4}	2.35	6.41 X 10^{-4}
	13.2	122.1-122.2	17.5	2.37 X 10^{-3}	3.47	2.02 X 10^{-3}
	16.8-17.3	119.8-121.9	17.1	4.20 X 10^{-3}	4.59	3.74 X 10^{-3}
D-6	7.4	147.0	28.8	3.15 X 10^{-4}	1.03	2.12 X 10^{-4}
	14.7	146.8-146.9	28.8	3.88 X 10^{-4}	2.07	1.81 X 10^{-4}
	21.6	146.6-146.7	28.7	4.40 X 10^{-4}	3.05	1.35 X 10^{-4}
	28.5	146.4	28.6	5.41 X 10^{-4}	4.04	1.37 X 10^{-4}
D-12	7.1	144.7-145.2	27.9	3.74 X 10^{-4}	1.04	2.70 X 10^{-4}
	14.2	144.6-144.7	27.8	4.73 X 10^{-4}	2.08	2.65 X 10^{-4}
	20.9	144.5-144.6	27.7	5.51 X 10^{-4}	3.07	2.44 X 10^{-4}
	27.5-27.6	144.3-144.5	27.6	6.91 X 10^{-4}	4.06	2.85 X 10^{-4}
E/J-2	6.4	136.6-136.7	25.1	3.97 X 10^{-4}	1.03	2.94 X 10^{-4}
	12.7-12.8	136.4-136.5	25.0	5.21 X 10^{-4}	2.06	3.15 X 10^{-4}
	18.8	136.2-136.3	24.9	9.10 X 10^{-4}	3.04	6.06 X 10^{-4}
	24.6-24.7	135.7-136.0	24.8	1.53 X 10^{-3}	4.02	2.75 X 10^{-3}
E/J-8	6.5	137.9-138.1	25.4	5.21 X 10^{-4}	1.03	4.13 X 10^{-4}
	12.9-13.0	137.7-137.9	25.3	6.54 X 10^{-4}	2.07	4.47 X 10^{-4}
	19.0	137.4-137.5	25.2	9.38 X 10^{-4}	3.05	6.33 X 10^{-4}
	25.0	137.0-137.4	25.2	1.55 X 10^{-3}	4.04	1.15 X 10^{-3}

DISTRIBUTION LIST

No. of Copies	To
1	Office of the Under Secretary of Defense for Research and Engineering, The Pentagon, Washington, DC 20301
12	Commander, Defense Technical Information Center, Cameron Station, Building 5, 5010 Duke Street, Alexandria, VA 22314
	Metals and Ceramics Information Center, Battelle Columbus Laboratories, 505 Avenue, Columbus, OH 43201
1	ATTN: Mr. Robert J. Fiorentino, Program Manager
	Defense Advanced Research Projects Agency, Defense Sciences Office/MSD, 1400 Boulevard, Arlington, VA 22209
1	ATTN: Dr. Steven G. Fishman
	Headquarters, Department of the Army, Washington, DC 20314
1	ATTN: DAEN-RDM, Mr. J. J. Healy
	Commander, U.S. Air Force Wright Aeronautical Laboratories, Wright-Patterson Air Force Base, OH 45433
1	ATTN: AFWAL/MLC
1	AFWAL/MLLP, D. M. Forney, Jr.
1	AFWAL/MLBC, Mr. Stanley Schulman
1	AFWAL/MLLS, Dr. Terence M. F. Ronald
1	AFWAL/FIBEC, Dr. Steve Johnson
1	Edward J. Morrissey, AFWAL/MLTE, Wright-Patterson Air Force Base, OH 45433
	Commander, Army Research Office, P.O. Box 12211, Research Triangle Park, NC 27709
1	ATTN: Information Processing Office
1	Dr. George Mayer
	Commander, U.S. Army Materiel Development and Readiness Command, 5001 Eisenhower Avenue, Alexandria, VA 22333
1	ATTN: DRCLD
	Commander, U.S. Army Armament, Munitions and Chemical Command, Dover, NJ 07801
1	ATTN: DRDAR-SCM, J. D. Corrie
1	Mr. Harry E. Pebly, Jr., PLASTEC, Director
	Commander, U.S. Army Aviation Research and Development Command, 4300 Goodfellow Blvd., St. Louis, MO 63120
1	ATTN: DRDAV-NS, Harold Law
	Director, U.S. Army Ballistic Research Laboratory, Aberdeen Proving Ground, MD 21005
1	ATTN: DRDAR-TSB-S (STINFO)

No. of Copies	To
	Commander, U.S. Army Electronics Research and Development Command, Fort Monmouth, NJ 07703
1	ATTN: DELSD-L
1	DELSD-E
	Commander, U.S. Army Foreign Science and Technology Center, 220 7th Street, N.E., Charlottesville, VA 22901
1	ATTN: Military Tech, Mr. Marley
	Commander, U.S. Army Materiel Systems Analysis Activity, Aberdeen Proving Ground, MD 21005
1	ATTN: DRXSY-MP, H. Cohen
	Commander, U.S. Army Missile Command, Redstone Arsenal, AL 35898
1	ATTN: Technical Library
1	DRSMI-RLM
1	DRSMI-RLA, Dr. James J. Richardson
	Commander, U.S. Army Mobility Equipment Research and Development Command, Fort Belvoir, VA 22060
1	ATTN: DRDME-D
1	DRDME-M
1	DRDME-MD
1	DRDME-V
	Commander, U.S. Army Research and Technology Labs, Applied Technology Laboratory (AVRADCOM), Fort Eustis, VA 23604
1	ATTN: DRDAR-ATL-ATP, Mr. James Gomez, Aerospace Engineer
	Commander, U.S. Army Tank-Automotive Command, Warren, MI 48090
1	ATTN: DRSTA-RCKM
	Director, Benet Weapons Laboratory, LCWSL, USA ARRADCOM, Watervliet, NY 12189
1	ATTN: DRSMC-LCB-TL
1	DRSMC-LCB-PS, Dr. I. Ahmad
	David Taylor Naval Ship Research and Development Center, Annapolis, MD 21402
1	ATTN: Dr. Michael Vassilaros - Code 2814
	Office of Naval Technology, 800 N. Quincy Street, Arlington, VA 20017
1	ATTN: Mr. J. J. Kelly - Code MAT 0715
	Naval Research Laboratory, Washington, DC 20375
1	ATTN: Dr. C. I. Chang - Code 5830
1	Dr. G. R. Yoder - Code 6384
	Chief of Naval Research, Arlington, VA 22217
1	ATTN: Code 471
	Naval Sea Systems Command, Washington, DC 20362
1	ATTN: Mr. Marlin Kinna - 62R4

No. of Copies	To
	Naval Surface Weapons Center, White Oak, Silver Spring, MD 20910
1	ATTN: John V. Foltz - Code R32
1	Dr. Herbert Newborn - Code R34
	National Aeronautics and Space Administration, Washington, DC 20546
1	ATTN: Mr. G. C. Deutsch - Code RW
1	Mr. Michael A. Greenfield, Program Manager for Materials, Code RTM-6
	National Aeronautics and Space Administration, Lewis Research Center, Cleveland, OH 44135
1	ATTN: Dr. James A. DiCarlo, Mail Stop 106-1
	National Aeronautics and Space Administration, Marshall Space Flight Center, Huntsville, AL 35812
1	ATTN: R. J. Schwinghammer, EH01, Dir, M&P Lab
1	Mr. W. A. Wilson, EH41, Bldg. 4612
	The Boeing Vertol Company, P.O. Box 16858, Philadelphia, PA 19142
1	ATTN: Mr. Robert L. Pinckney, Mail Stop P62-06
1	Mr. Joseph W. Lenski, Jr., Mail Stop P32-09
	E. I. DuPont De Nemours and Company, Inc., Textile Fibers Department, Pioneering Research Laboratory, Experimental Station, Wilmington, DE 19898
1	ATTN: Blake R. Bichlmeir
1	Mr. Rex C. Claridge, TRW, Incorporated, Manufacturing Division, Mail Stop 01-2210, 1 Space Park, Redondo Beach, CA 90278
1	Dr. Bhagwam K. Das, Engineering Technology Supervisor, The Boeing Company, P.O. Box 3999, Seattle, WA 98124
1	Leroy Davis, NETCO, 2225 East 28th Street, Building 5, Long Beach, CA 90806
1	Louis A. Gonzales, Kaman Tempo, 816 State Street, Santa Barbara, CA 93101
1	Mr. Joseph F. Dolowy, Jr., President, DWA Composite Specialties, Inc., 21133 Superior Street, Chatsworth, CA 91311
1	Prof. G. J. Dvorak, Civil Engineering Department, University of Utah, Salt Lake City, UT 84112
1	Mr. Robert E. Fisher, President, AMERCOM, Inc., 8948 Fullbright Avenue, Chatsworth, CA 91311
1	William F. Grant, AVCO Specialty Materials Division, 2 Industrial Avenue, Lowell, MA 01851
1	Mr. Jacob Gubbay, Charles Stark Draper Laboratories, 555 Technology Square, Mail Station 27, Cambridge, MA 02139

No. of Copies	To
1	Mr. John E. Hack, Southwest Research Institute, 6220 Culebra Road, San Antonio, TX 78284
1	Dr. H. A. Katzman, The Aerospace Corporation, P.O. Box 92957 Los Angeles, CA 90009
	Lockheed California Company, Burbank, CA 91520
1	ATTN: Mr. Rod F. Simenz, Department of Materials and Processes
	Lockheed Georgia Company, 86 South Cobb Drive, Marietta, GA 30063
1	ATTN: Materials and Processes Engineering Department
1	Mr. James Carroll
1	Mr. Patrick J. Moore, Staff Engineer, Lockheed Missiles and Space Company, Organization 62-60, Building 104, P.O. Box 504, Sunnyvale, CA 94086
1	R. Byron Pipes, Professor & Director, Center for Composite Materials, University of Delaware, Newark, DE 19711
1	Dr. Karl M. Prewo, Principal Scientist, United Technologies Research Center, Mail Stop 24, East Hartford, CT 06108
1	Dr. B. W. Rosen, Materials Sciences Corporation, Gwynedd Plaza 11, Bethlehem Pike, Spring House, PA 19477
1	Prof. Marc H. Richman, Division of Engineering, Brown University, Providence, RI 02912
1	Mr. Ronald P. Tye, Energy Materials Testing Laboratory, Biddeford Industrial Park, Biddeford, ME 04005
1	Mr. Robert C. Van Siclen, Vought Corporation, Advanced Technology Center, P.O. Box 226144, Dallas, TX 75266
1	Prof. Franklin E. Wawner, Department of Materials Science, School of Engineering and Applied Sciences, University of Virginia, Charlottesville, VA 22903
1	Dr. Carl Zweben, General Electric Company, Valley Forge Space Center/M4018, P.O.Box 8555, Philadelphia, PA 19101
1	Prof. James G. Goree, Dept. of Mechanical Engineering, Clemson University, Clemson, SC 29631
	Director, Army Materials and Mechanics Research Center, Watertown, MA 02172
2	ATTN: DRXMR-PL
1	DRXMR-PAT
1	DRXMR-K
8	DRXMR-MMC, Mr. J. Nunes

Army Materials and Mechanics Research Center, Watertown, MA 02172
LOSS FACTORS MEASURED IN METAL MATRIX COMPOSITES
Nancy S. Timmerman & John Doherty
Bolt Beranek and Newman Inc.
Technical Report AMMRC TR 84-22
June 1984, 64 pp.
illus - tables, Contract
No. DAAG46-82-C-0060

AD ____________
Unclassified
Unlimited Distribution

Key Words

Metal matrix composites
Damping
Graphite
Silicon carbide
Aluminum
Magnesium
Alumina

The resonant dwell technique was used to measure loss factors at the fundamental frequency of a number of cantilever beam samples (100 to 200 Hz). Nine different metral matrix composites, three unreinforced base metals, and eight configurations of FP(AL_2O_3)/ZE41AMg were tested at three temperatures and four peak sample stress levels below 30,000 psi. The results indicate increasing loss factor with increasing stress level. Loss factors of all composites except graphite/aluminum composites were lower than those of the corresponding base metal. For FP/ZE41AMg composites, higher losses were observed with heat treatment, lower fiber volume fraction, and $\pm 22\frac{1}{2}^{\circ}$ fiber orientation. Trends of loss factor with temperature varied with material type.

Army Materials and Mechanics Research Center, Watertown, MA 02172
LOSS FACTORS MEASURED IN METAL MATRIX COMPOSITES
Nancy S. Timmerman & John Doherty
Bolt Beranek and Newman Inc.
Technical Report AMMRC TR 84-22
June 1984, 64 pp.
illus - tables, Contract
No. DAAG46-82-C-0060

AD ____________
Unclassified
Unlimited Distribution

Key Words

Metal matrix composites
Damping
Graphite
Silicon carbide
Aluminum
Magnesium
Alumina

The resonant dwell technique was used to measure loss factors at the fundamental frequency of a number of cantilever beam samples (100 to 200 Hz). Nine different metral matrix composites, three unreinforced base metals, and eight configurations of FP(AL_2O_3)/ZE41AMg were tested at three temperatures and four peak sample stress levels below 30,000 psi. The results indicate increasing loss factor with increasing stress level. Loss factors of all composites except graphite/aluminum composites were lower than those of the corresponding base metal. For FP/ZE41AMg composites, higher losses were observed with heat treatment, lower fiber volume fraction, and $\pm 22\frac{1}{2}^{\circ}$ fiber orientation. Trends of loss factor with temperature varied with material type.

Army Materials and Mechanics Research Center, Watertown, MA 02172
LOSS FACTORS MEASURED IN METAL MATRIX COMPOSITES
Nancy S. Timmerman & John Doherty
Bolt Beranek and Newman Inc.
Technical Report AMMRC TR 84-22
June 1984, 64 pp.
illus - tables, Contract
No. DAAG46-82-C-0060

AD ____________
Unclassified
Unlimited Distribution

Key Words

Metal matrix composites
Damping
Graphite
Silicon carbide
Aluminum
Magnesium
Alumina

The resonant dwell technique was used to measure loss factors at the fundamental frequency of a number of cantilever beam samples (100 to 200 Hz). Nine different metral matrix composites, three unreinforced base metals, and eight configurations of FP(AL_2O_3)/ZE41AMg were tested at three temperatures and four peak sample stress levels below 30,000 psi. The results indicate increasing loss factor with increasing stress level. Loss factors of all composites except graphite/aluminum composites were lower than those of the corresponding base metal. For FP/ZE41AMg composites, higher losses were observed with heat treatment, lower fiber volume fraction, and $\pm 22\frac{1}{2}^{\circ}$ fiber orientation. Trends of loss factor with temperature varied with material type.

Army Materials and Mechanics Research Center, Watertown, MA 02172
LOSS FACTORS MEASURED IN METAL MATRIX COMPOSITES
Nancy S. Timmerman & John Doherty
Bolt Beranek and Newman Inc.
Technical Report AMMRC TR 84-22
June 1984, 64 pp.
illus - tables, Contract
No. DAAG46-82-C-0060

AD ____________
Unclassified
Unlimited Distribution

Key Words

Metal matrix composites
Damping
Graphite
Silicon carbide
Aluminum
Magnesium
Alumina

The resonant dwell technique was used to measure loss factors at the fundamental frequency of a number of cantilever beam samples (100 to 200 Hz). Nine different metral matrix composites, three unreinforced base metals, and eight configurations of FP(AL_2O_3)/ZE41AMg were tested at three temperatures and four peak sample stress levels below 30,000 psi. The results indicate increasing loss factor with increasing stress level. Loss factors of all composites except graphite/aluminum composites were lower than those of the corresponding base metal. For FP/ZE41AMg composites, higher losses were observed with heat treatment, lower fiber volume fraction, and $\pm 22\frac{1}{2}^{\circ}$ fiber orientation. Trends of loss factor with temperature varied with material type.

Army Materials and Mechanics Research Center, Watertown, MA 02172
LOSS FACTORS MEASURED IN METAL MATRIX COMPOSITES
Nancy S. Timmerman & John Doherty
Bolt Beranek and Newman Inc.
Technical Report AMMRC TR 84-22
June 1984, 64 pp. illus - tables, Contract No. DAAG46-82-C-0060

AD ____________
Unclassified
Unlimited Distribution

Key Words

Metal matrix composites
Damping
Graphite
Silicon carbide
Aluminum
Magnesium
Alumina

The resonant dwell technique was used to measure loss factors at the fundamental frequency of a number of cantilever beam samples (100 to 200 Hz). Nine different metral matrix composites, three unreinforced base metals, and eight configurations of FP(AL_2O_3)/ZE41AMg were tested at three temperatures and four peak sample stress levels below 30,000 psi. The results indicate increasing loss factor with increasing stress level. Loss factors of all composites except graphite/aluminum composites were lower than those of the corresponding base metal. For FP/ZE41AMg composites, higher losses were observed with heat treatment, lower fiber volume fraction, and $\pm 22\frac{1}{2}^{\circ}$ fiber orientation. Trends of loss factor with temperature varied with material type.

Army Materials and Mechanics Research Center, Watertown, MA 02172
LOSS FACTORS MEASURED IN METAL MATRIX COMPOSITES
Nancy S. Timmerman & John Doherty
Bolt Beranek and Newman Inc.
Technical Report AMMRC TR 84-22
June 1984, 64 pp. illus - tables, Contract No. DAAG46-82-C-0060

AD ____________
Unclassified
Unlimited Distribution

Key Words

Metal matrix composites
Damping
Graphite
Silicon carbide
Aluminum
Magnesium
Alumina

The resonant dwell technique was used to measure loss factors at the fundamental frequency of a number of cantilever beam samples (100 to 200 Hz). Nine different metral matrix composites, three unreinforced base metals, and eight configurations of FP(AL_2O_3)/ZE41AMg were tested at three temperatures and four peak sample stress levels below 30,000 psi. The results indicate increasing loss factor with increasing stress level. Loss factors of all composites except graphite/aluminum composites were lower than those of the corresponding base metal. For FP/ZE41AMg composites, higher losses were observed with heat treatment, lower fiber volume fraction, and $\pm 22\frac{1}{2}^{\circ}$ fiber orientation. Trends of loss factor with temperature varied with material type.

Army Materials and Mechanics Research Center, Watertown, MA 02172
LOSS FACTORS MEASURED IN METAL MATRIX COMPOSITES
Nancy S. Timmerman & John Doherty
Bolt Beranek and Newman Inc.
Technical Report AMMRC TR 84-22
June 1984, 64 pp. illus - tables, Contract No. DAAG46-82-C-0060

AD ____________
Unclassified
Unlimited Distribution

Key Words

Metal matrix composites
Damping
Graphite
Silicon carbide
Aluminum
Magnesium
Alumina

The resonant dwell technique was used to measure loss factors at the fundamental frequency of a number of cantilever beam samples (100 to 200 Hz). Nine different metral matrix composites, three unreinforced base metals, and eight configurations of FP(AL_2O_3)/ZE41AMg were tested at three temperatures and four peak sample stress levels below 30,000 psi. The results indicate increasing loss factor with increasing stress level. Loss factors of all composites except graphite/aluminum composites were lower than those of the corresponding base metal. For FP/ZE41AMg composites, higher losses were observed with heat treatment, lower fiber volume fraction, and $\pm 22\frac{1}{2}^{\circ}$ fiber orientation. Trends of loss factor with temperature varied with material type.

Army Materials and Mechanics Research Center, Watertown, MA 02172
LOSS FACTORS MEASURED IN METAL MATRIX COMPOSITES
Nancy S. Timmerman & John Doherty
Bolt Beranek and Newman Inc.
Technical Report AMMRC TR 84-22
June 1984, 64 pp. illus - tables, Contract No. DAAG46-82-C-0060

AD ____________
Unclassified
Unlimited Distribution

Key Words

Metal matrix composites
Damping
Graphite
Silicon carbide
Aluminum
Magnesium
Alumina

The resonant dwell technique was used to measure loss factors at the fundamental frequency of a number of cantilever beam samples (100 to 200 Hz). Nine different metral matrix composites, three unreinforced base metals, and eight configurations of FP(AL_2O_3)/ZE41AMg were tested at three temperatures and four peak sample stress levels below 30,000 psi. The results indicate increasing loss factor with increasing stress level. Loss factors of all composites except graphite/aluminum composites were lower than those of the corresponding base metal. For FP/ZE41AMg composites, higher losses were observed with heat treatment, lower fiber volume fraction, and $\pm 22\frac{1}{2}^{\circ}$ fiber orientation. Trends of loss factor with temperature varied with material type.